Determination of the charm- and beauty-quark masses from QCD sum rules

G.R. Gluckman

B.Sc., University of Cape Town (1991)
B.Sc.(Hons), University of Cape Town (1992)

Submitted in partial fulfilment
of the requirements for the degree of

Master of Science

at the

UNIVERSITY OF CAPE TOWN

August 9, 1994

Contents

Abstract

Ratios of Laplace QCD sum rules are used in order to determine the on-shell charm- and beauty-quark masses. After confronting the experimental data in the charmonium and bottonium systems with theory, we obtain $m_c = 1.46 \pm 0.07\, GeV$ *and* $m_b = 4.70 \pm 0.07\, GeV$. *The error is due to the uncertainties in the values of* Λ *and the gluon condensate.*

Chapter 1

QCD

1.1 Introduction

The most successful Quantum Field Theory to-date is Quantum Electrodynamics (QED) [1]. QED describes the interaction of photons with matter, such as the behavior of particles like the electron and muon whose dominant interactions are electromagnetic. One of the major reasons for the success of QED lies in the fact that precise measurements of many electromagnetic observables have been matched with theoretical perturbative approximations, agreeing to a few parts in a million.

Quantum Chromodynamics (QCD) [2, 3], on the other hand, is the theory which describes strong interactions. It is a non-abelian gauge theory, describing the interaction of the color degree of freedom of the quarks with massless gauge fields, the gluons. There are six quarks with flavors : up, down, strange, charm, bottom (or beauty) and top (or truth), and they each come in three colors : say, red, green and blue. So far, there has been experimental evidence for the existence of the five lightest quarks, the top-quark is still intensively being sought.

In analogy with the photon, which is the abelian gauge field mediating the electromagnetic interaction between charged particles in QED, the gluon is a non-abelian gauge field in QCD and it mediates color interactions between quarks. Unlike the photon which carries no charge (i.e it is neutral), the gluon carries color charges and can thus interact with each other. This direct gluon-gluon coupling makes QCD far richer than QED, as well as far more complicated. It allows for the possibility of *glueballs*, which are bound states of gluons without the need for any quarks being present.

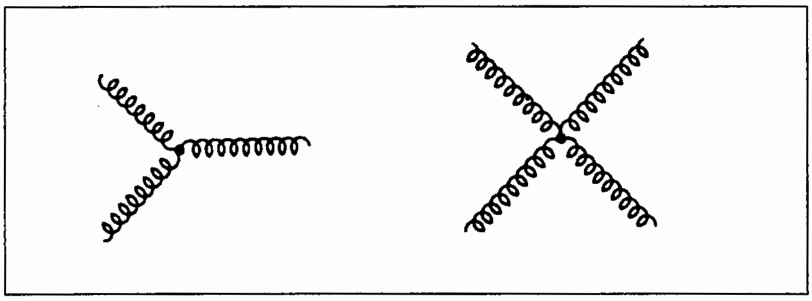

Figure 1.1: This direct gluon-gluon coupling allows for the possibility of *glueballs*.

Since we do not see colored particles, one can assume that hadronic matter is unaltered under the exchange of colors. One can thus choose a corresponding group $SU(3)_c$, so that physical phenomena are invariant under transformations, corresponding to all hadron states and physical observables being color-singlets.

In the 50's and 60's, a perturbative approach was not thought possible for the theory of strong interactions. This was due to the size of the coupling constant. By looking at the forces between two protons, experimentally $g^2/4\pi$ was determined to be larger than unity, thus rendering any perturbative approach useless. This plagued particle physics for years, as unlike in QED where the importance of higher order Feynman diagrams become less important, the converse was the case for strong interactions. The great triumph of QCD came in 1973, when it was discovered that the coupling constant was not constant at all, but in fact depends on the separation distance between the interacting particles. At large distances α_s is large, but at short distances (less than the size of the proton) it becomes quite small. This phenomenon is known as *Asymptotic freedom.* Although a perturbative approach is now possible for small distances, most physical observables we would like to explain (such as the hadron spectrum), rely on looking at regions of large α_s, thus calling for non-perturbative phenomena.

1.1.1 Indirect evidence for quarks & color

There are several well-known experiments which give indirect evidence for the existence of quarks, gluons and the color degrees of freedom. In the e^+e^- annihilation experiment, one considers very high-energy e^+e^- collisions, where annihilation into hadrons is the dominant process.[1] The ratio for the cross-section $\sigma(e^+e^- \rightarrow hadrons)$ and the cross-section $\sigma(e^+e^- \rightarrow \mu^+\mu^-)$ is theoretically given as

$$R = \frac{\sigma(e^+e^- \rightarrow hadrons)}{\sigma(e^+e^- \rightarrow \mu^+\mu^-)} = N_c \sum_{i=1}^{N_f} Q_i^2 \tag{1.1}$$

and can be seen to be directly related to the number of color degrees of freedom N_c. For $N_c = 3$ and the energy regions $\sqrt{s} < 3$ GeV, 4 GeV $< \sqrt{s} < 9$ GeV and $\sqrt{s} > 10$ GeV the ratio $R = 2$, $10/3$ and $11/3$ respectively. This matches well with experiment as can be seen in Fig. 1.2.

The other well-know process is $\pi^0 \rightarrow 2\gamma$. The decay rate for this process can be calculated by taking into account the contribution from the lowest order Feynman diagram yielding

$$\Gamma\left(\pi^0 \rightarrow 2\gamma\right) = N_c^2 \left(Q_u^2 - Q_d^2\right)^2 \frac{\alpha^2 m_{\pi^0}^3}{64\pi^3 F_\pi^2}. \tag{1.2}$$

With $N_c = 3$, experiment and theory agree extremely well with each other.

[1]The hadron formation is really at the next level following $e^+e^- \rightarrow \bar{q}q$. The pair production of almost free-quarks is followed by a hadronization process.

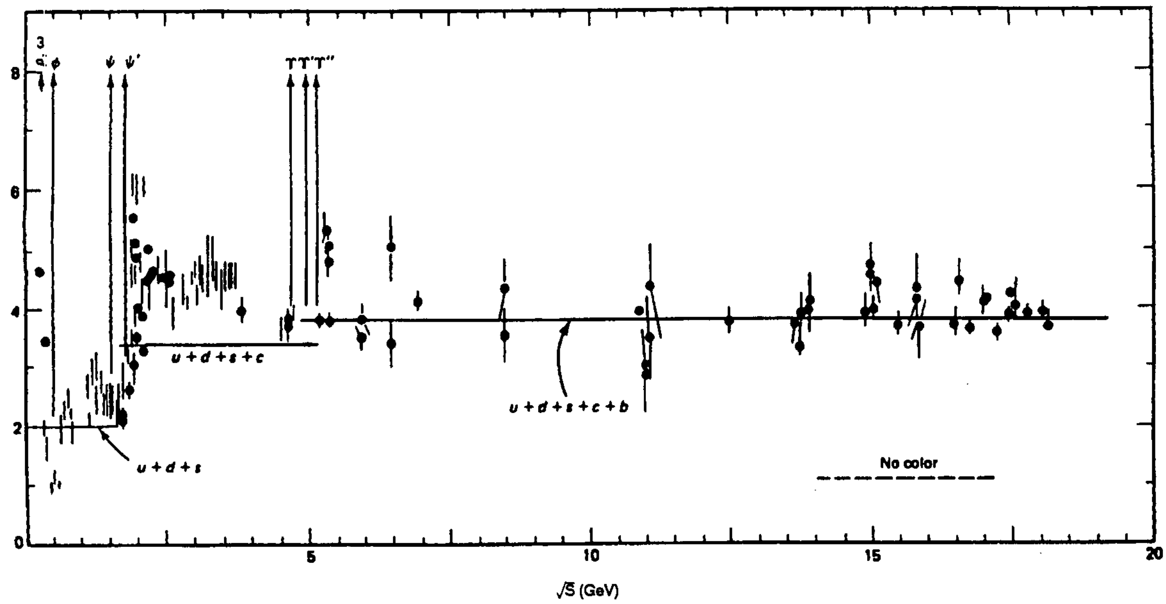

Figure 1.2: The ratio (1.1) compared to experimental data is plotted against electron energy (in GeV), from *Introduction to Elementary Particle Physics*, D. Griffiths, (New York: Wiley, ©1987, p. 263).

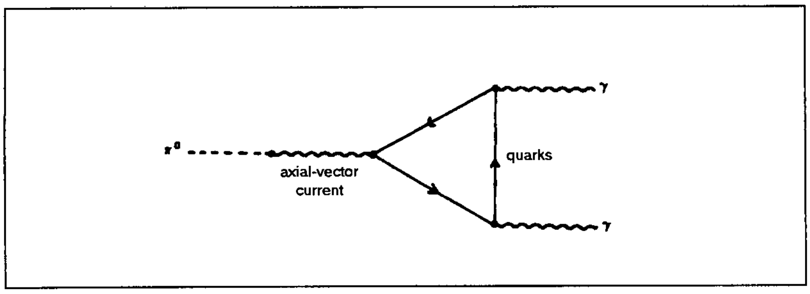

Figure 1.3: Lowest order Feynman diagram for $\pi^0 \rightarrow 2\gamma$.

There is also good evidence for quarks from experiments on deep inelastic scattering of electrons off protons. From this it has been revealed that electrons are in fact scattering off point-like constituents within the proton, i.e. quarks.[2]

Also, 3-jet events have been observed. This can be interpreted as evidence for gluons. The 3-jet events occur from the quark-gluon bremsstrahlung as shown in the following picture.

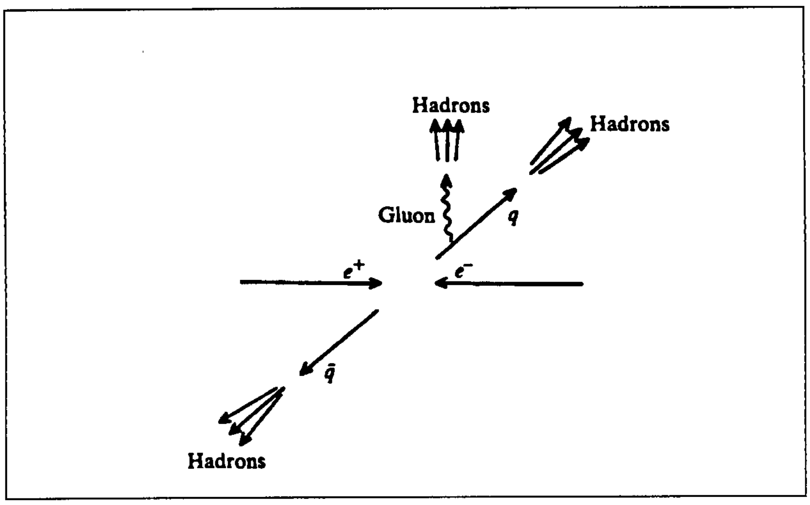

Figure 1.4: A 3-jet event.

[2]Bjorken and Feynman referred to them as partons.

1.2 QCD Lagrangian

There are several reasons for believing that QCD is the best candidate for the theory of strong interactions, even though confinement is still unexplained. The QCD Lagrangian is

$$\begin{aligned}\mathcal{L}_{QCD} &= -\frac{1}{4}G_{\mu\nu}^{(a)}(x)\,G_{(a)}^{\mu\nu}(x) - \frac{1}{2a}\partial_\mu W_{(a)}^{\mu}(x)\,\partial^\nu W_\nu^{(a)}(x) \\ &\quad -\partial_\mu\bar{\varphi}_{(a)}(x)\left[\delta_{ab}\partial^\mu - ig\left(-if_{cab}\right)W_{(c)}^{\mu}(x)\right]\varphi_{(b)}(x) \\ &\quad +i\sum_{j=1}^{N_f}\bar{\psi}_j^{\alpha}(x)\,\gamma^\mu\left[\delta_{\alpha\beta}\partial_\mu - ig\sum_{a=1}^{8}\tfrac{1}{2}\lambda_{\alpha\beta}^{(a)}W_\mu^{(a)}(x)\right]\psi_j^{\beta}(x) \\ &\quad -\sum_{j=1}^{N_f}m_j\bar{\psi}_j^{\alpha}(x)\,\psi_{\alpha j}(x)\end{aligned} \tag{1.3}$$

where in (1.3),

$$G_{\mu\nu}^{(a)}(x) = \partial_\mu W_\nu^{(a)}(x) - \partial_\nu W_\mu^{(a)}(x) + gf_{abc}W_\mu^{(b)}(x)\,W_\nu^{(c)}(x) \tag{1.4}$$

is the Yang-Mills field strength constructed from the gluon fields $W_\mu^{(a)}(x)$ with μ,ν been the space-time indices and $a = 1, 2, \ldots, 8$ corresponds to the 8 gluon fields.[3] The $\psi_j^\alpha(x)$ are 4-component Dirac spinors with color indices α, β =red, green and blue, and flavor indices j = up, down, strange, charm,..., N_f. The $\varphi_{(a)}$ are eight anti-commuting scalar fields in the $\underline{8}$ representation of $SU(3)$. The QCD coupling constant is g and f_{abc} are the structure constants of the $SU(3)$ algebra

$$\left[T^{(a)}, T^{(b)}\right] = if_{abc}T^{(c)} \tag{1.5}$$

where $T^{(a)}$ are the generators of the $SU(3)$ algebra. In the fundamental $\underline{3}$ dimensional representation, the generators of $SU(3)$ are[4]

$$\left(T^{(a)}\right)_{\alpha\beta} = \tfrac{1}{2}\lambda_{\alpha\beta}^{(a)} \tag{1.6}$$

[3]This should not be confused with the coupling a in the gauge-fixing term.
[4]Corresponding to the color basis of the quark fields.

where $\lambda^{(a)}_{\alpha\beta}$ are the 3×3 Gell-Mann matrices. In the regular (adjoint) $\underline{8}$ dimensional representation[5]

$$\left(T^{(a)}\right)_{bc} = -if_{abc} \tag{1.7}$$

1.2.1 Global Symmetry properties

The QCD Lagrangian defined in (1.3) is invariant under

$$\psi\left(x\right) \rightarrow \exp\left(-i\theta\hat{1}\right)\psi\left(x\right) \tag{1.8}$$

where $\hat{1}$ is the unit matrix. There is an associated conserved current,[6] the baryonic current

$$J^{\mu}\left(x\right) = \sum_{j=1}^{N_f} \bar{\psi}_j\left(x\right)\gamma^{\mu}\psi_j\left(x\right) \tag{1.9}$$

and its associated charge

$$B = \int d^3x J^0\left(\vec{x}, t\right) \tag{1.10}$$

the generator of a $U_B\left(1\right)$ group. The Lagrangian defined in (1.3) also has a $U_1\left(1\right)\otimes U_2\left(1\right)\otimes \ldots U_{N_f}\left(1\right)$ global symmetry, that is to say it is invariant under the global transformations:

$$\psi_j\left(x\right) \rightarrow \exp\left(-i\theta_j\hat{1}\right)\psi_j\left(x\right) \tag{1.11}$$

which acts on the quark flavor components. Furthermore, in the massless limit $\mathcal{L}_{QCD}$ is invariant under the transformation

$$\psi_j\left(x\right) \rightarrow \exp\left(-i\theta\hat{1}\gamma_5\right)\psi_j\left(x\right) \tag{1.12}$$

acting on flavor components, with a corresponding axial baryonic current

$$J_5^{\mu}\left(x\right) = \sum_{j=1}^{N_f} \bar{\psi}_j\left(x\right)\gamma^{\mu}\gamma_5\psi_j\left(x\right). \tag{1.13}$$

[5]Corresponding to the gluon basis.
[6]Conserved current via Noether's theorem.

Setting the masses of different flavored quarks to be equal, i.e.

$$m_1 = m_2 = \ldots = m_{N_f} \tag{1.14}$$

then the $U_1(1) \otimes U_2(1) \otimes \ldots U_{N_f}(1)$ invariance is enlarged to a global $SU(N_f)$ symmetry. If the masses of all the flavors are zero, then $\mathcal{L}_{QCD}$ is invariant under the transformation

$$\psi(x) \to \exp\left(-i\theta^{(A)}T^{(A)}\right)\psi(x) \tag{1.15}$$

where $\theta^{(A)}$ are constant parameters and $T^{(A)}$ are the infinitesimal generators $SU(N_f)$. The corresponding conserved current is

$$V_\mu^{(A)}(x) = \bar{\psi}^i(x)\gamma_\mu T_{ij}^{(A)}\psi^j(x) \tag{1.16}$$

and the associated charge

$$Q^{(A)} = \int d^3x V_0(\vec{x}, t). \tag{1.17}$$

In addition, in the massless limit, $\mathcal{L}_{QCD}$ is invariant under the transformation

$$\psi(x) \to \exp\left(-i\theta_5^{(A)}T^{(A)}\gamma_5\right)\psi(x) \tag{1.18}$$

with a corresponding conserved current

$$A_\mu^{(A)}(x) = \bar{\psi}^i(x)\gamma_\mu\gamma_5 T_{ij}^{(A)}\psi^j(x) \tag{1.19}$$

and an associated charge

$$Q_5^{(A)} = \int d^3x A_0(\vec{x}, t). \tag{1.20}$$

$V_\mu^{(A)}(x)$ and $A_\mu^{(A)}(x)$ above, are the vector and axial-vector currents of the algebra of currents of Gell-Mann. Also, the combination of charges

$$Q_L^{(A)} = Q^{(A)} - Q_5^{(A)} \tag{1.21}$$

$$Q_R^{(A)} = Q^{(A)} + Q_5^{(A)} \tag{1.22}$$

are generators of chiral $SU_L(N_f) \otimes SU_R(N_f)$ and are conserved in the massless limit.

1.2.2 The B-R-S transformations

The full Lagrangian (1.3) is not gauge invariant as a result of the added gauge fixing term, but there is a generalization of gauge invariance, the so called Becchi-Rouet-Stora (or B-R-S) invariance. The B-R-S transformations are

$$W_\mu^{(a)}(x) \to W_\mu'^{(a)}(x) = W_\mu^{(a)}(x) + \omega\left(D_\mu\varphi\right)^{(a)}(x) \tag{1.23}$$

$$\psi(x) \to \psi'(x) = \exp\left(-ig\omega\vec{T}\cdot\vec{\varphi}(x)\right)\psi(x) \tag{1.24}$$

$$\bar{\varphi}^{(a)}(x) \to \bar{\varphi}'^{(a)}(x) = \bar{\varphi}^{(a)}(x) + \frac{\omega}{a}\partial^\mu W_\mu^{(a)}(x) \tag{1.25}$$

$$\varphi^{(a)}(x) \to \varphi'^{(a)}(x) = \varphi^{(a)}(x) - \frac{1}{2}g\omega\varphi^{(b)}(x)\, f_{abc}\varphi^{(c)}(x) \tag{1.26}$$

and all the relations among the Green's functions which result from local gauge invariance, the Slavnov-Taylor identities, are generated by the above B-R-S transformations.

1.3 Regularization & Renormalization

In QCD, it is straightforward to calculate the self-energy or vertex diagrams at tree level, but as soon as one or more loops are added, results of calculations of the Feynman diagrams become infinite due to ultra-violet divergences. To circumvent this problem, one needs to renormalize the theory. The steps involved in constructing a renormalizable theory are as follows:

1. Regularizing the unrenormalized Green's functions in a manner which preserves the Slavnov-Taylor identities. One way to regularize the theory, is to use the so-called dimensional regularization [4, 5, 6]. One begins by reducing the number of space-time dimensions from $D = 4$ to $D = 4 - \epsilon$. This forces one to redefine the Dirac algebra in $D = 4 - \epsilon$ dimensions, as well as change the dimensions of the fields, coupling constants, gauge parameters and masses.

2. Identifying the primitive divergences.

3. Performing one-loop renormalization subtractions which render the primitive divergences finite. These subtractions are again constrained by the Slavnov-Taylor identities.

4. These subtractions are formally achieved by adding counter terms to the initial Lagrangian. These counter terms exactly cancel the divergent parts of the theory, so

$$\mathcal{L}_{QCD} \rightarrow \mathcal{L}_{QCD} + \Delta\mathcal{L}_{QCD}$$

and to each term there is a corresponding subtraction term added Δ_i, which are taken as a power series in α_s, where

$$\alpha_s = \frac{g^2}{4\pi}\left(\nu^2\right)^{-\epsilon/2} \tag{1.27}$$

and ν is an arbitrary mass scale parameter. Furthermore, by writing $Z_i = 1 - \Delta_i$, it is possible to rescale the fields, coupling constant, gauge parameters and masses so that one may write the renormalized QCD Lagrangian as

$$\begin{aligned} \mathcal{L}_{QCD} &= -\frac{1}{4}\vec{G}^0_{\mu\nu}\cdot\vec{G}^{\mu\nu}_0 - \frac{1}{2a_0}\partial_\mu\vec{W}^\mu_0\cdot\partial^\nu\vec{W}^0_\nu - \partial_\mu\vec{\bar{\varphi}}_0\cdot D^\mu_0\vec{\varphi}_0 \\ &+\frac{i}{2}\sum_{j=1}^{N_f}\bar{\psi}_{j0}\gamma^\mu D^0_\mu\psi_{j0} - \sum_{j=1}^{N_f} m_{j0}\bar{\psi}_{j0}\psi_{j0}. \end{aligned} \tag{1.28}$$

There are a number of schemes used for subtracting these divergences. In the minimal subtraction scheme (MS scheme), the renormalization constants Z_i are chosen to cancel the poles in $1/\epsilon$ in the propagators. In the modified minimal subtraction scheme ($\overline{MS}$), terms of the form $(1/\epsilon - \ln 4\pi + \gamma)$ are subtracted in the propagators. In the μ-scheme, the Green's functions are subtracted at euclidean values of their invariants, and in the Weinberg mass-independent scheme (W-renormalization), the renormalization constants are obtained from the unrenormalized Green's functions which are evaluated at some euclidean value with their masses set to zero.

1.4 The Renormalization Group Equations (RGE)

The physical observables must be independent of the subtraction procedure. This invariance is called the Renormalization Group invariance and gives rise to the Renormalization Group Equations (RGE) [7]. If one uses a particular renormalization scheme, R, then the renormalized Green's functions Γ and the bare Green's functions Γ_0 are related to one another through

$$\Gamma\left(p_1,\ldots,p_N;\alpha_s,a,m_i,\mu\right) = Z_R\left(\mu,\epsilon\right)\Gamma_0\left(p_1,\ldots,p_N;\alpha_s^0,a^0,m_i^0,\epsilon\right) \tag{1.29}$$

where $Z_R\left(\mu,\epsilon\right)$ denotes the appropriate product of renormalization constants defined in the scheme which has been chosen.

Using (1.29) as a starting point, and performing chain differentiation, one can derive the fundamental equation of the renormalization group:

$$\begin{aligned} &\left\{-\frac{\partial}{\partial t}+\beta\left(\alpha_s\right)\alpha_s\frac{\partial}{\partial\alpha_s}+\beta_a\left(\alpha_s\right)\frac{\partial}{\partial a}\right. \\ &\left.-\sum_i\left[1+\gamma_i\left(\alpha_s\right)\right]x_i\frac{\partial}{\partial x_i}+D-\gamma_\Gamma\left(\alpha_s\right)\right\} \\ &\cdot\Gamma\left(e^t p_1,\ldots,e^t p_N;\alpha_s,a,x_i,\mu\right) = 0 \end{aligned} \tag{1.30}$$

where

$$x_i = m_i/\mu \tag{1.31}$$

$$\alpha_s\beta\left(\alpha_s\right) = \mu\frac{d\alpha_s}{d\mu} \tag{1.32}$$

$$-\gamma_i\left(\alpha_s\right) = \frac{\mu}{m_i}\frac{dm_i}{d\mu} \tag{1.33}$$

$$\beta_a\left(\alpha_s\right) = \mu\frac{da}{d\mu} \tag{1.34}$$

and D is the dimension of the Green's function in mass units. The function γ_Γ is often called the anomalous dimension, and is related to the number of external gluon, quark and ghost lines. The general solution to the fundamental equation can be obtained after solving the differential equations for the running coupling constant, mass, and gauge parameter:

$$\frac{d\bar{\alpha}_s(t,\alpha_s)}{dt} = \bar{\alpha}_s\beta(\bar{\alpha}_s) \quad , \quad \bar{\alpha}_s(0,\alpha_s) = \alpha_s \tag{1.35}$$

$$\frac{d\bar{x}_i(t,\alpha_s)}{dt} = -[1+\gamma_i(\bar{\alpha}_s)]\,\bar{x}_i \quad , \quad \bar{x}_i(0,\alpha_s) = x_i \tag{1.36}$$

$$\frac{d\bar{a}(t,\alpha_s)}{dt} = \beta_a(\bar{\alpha}_s) \quad , \quad \bar{a}(0,\alpha_s) = a \tag{1.37}$$

and then the general solution to the fundamental equation is

$$\Gamma\left(e^t p_1,\ldots,e^t p_N;\alpha_s,a,x_i,\mu\right) = \Gamma\left(p_1,\ldots,p_N;\bar{\alpha}_s,\bar{a},\bar{x}_i,\mu\right) \cdot \exp\left\{tD - \int_0^t dt'\gamma_\Gamma\left[\bar{\alpha}_s(t',\alpha_s)\right]\right\}. \tag{1.38}$$

The solution to the differential equation to two-loops for the running coupling constant is

$$\bar{\alpha}_s\left(-q^2\right) = \bar{\alpha}_s^{(2)}\left(\frac{q^2}{\Lambda^2}\right)\left\{1 - \frac{\bar{\alpha}_s^{(2)}}{\pi}\frac{\beta_2}{\beta_1}\ln\ln\left(-\frac{q^2}{\Lambda^2}\right)\right\} \tag{1.39}$$

where

$$\bar{\alpha}_s^{(2)}\left(\frac{q^2}{\Lambda^2}\right) = -\frac{2\pi}{\beta_1\ln\left(-q^2/\Lambda^2\right)} \tag{1.40}$$

and $\beta_{1,2}$ depend on the number of flavors

$$\beta_1 = \frac{1}{2}\left(-11 + \frac{2}{3}N_f\right) \tag{1.41}$$

$$\beta_2 = \frac{1}{4}\left(51 - \frac{19}{3}N_f\right). \tag{1.42}$$

Similarly for the running mass

$$\bar{m}_i\left(-q^2\right) = \bar{m}^{(2)}\left\{1 + \left(\gamma_1\frac{\beta_2}{\beta_1^2}\ln\ln\left(-q^2/\Lambda^2\right) - \frac{1}{\beta_1}\left(\gamma_2 - \gamma_1\frac{\beta_2}{\beta_1}\right)\right)\frac{\bar{\alpha}_s^{(2)}}{\pi}\right\} \tag{1.43}$$

where

$$\bar{m}^{(2)} = \hat{m}_i/\left(\frac{1}{2}\ln\left(-q^2/\Lambda^2\right)\right)^{-\gamma_1/\beta_1} \tag{1.44}$$

$$\gamma_1 = 2 \tag{1.45}$$

$$\gamma_2 = \frac{1}{6}\left(\frac{101}{2} - \frac{5}{3}N_f\right) \tag{1.46}$$

and $\hat{m}_i$ is the invariant mass.

Chapter 2

QCD sum rules

2.1 Introduction

By now it is well established that quarks form the building blocks for the observed array of hadrons. The quarks are weakly interacting at short distances, but strongly interacting at large distances giving rise to the bound states. One believes that at short distances the interactions between the quarks are mediated solely by the vector gluons coupled to color. At large distances the forces are extremely large and when the quarks separate, the extremely large force is screened through the creation of mesons. The short distance problem in QCD is relatively simple as Asymptotic freedom prevails and this allows one to perform meaningful perturbative calculations for solving the problem. The bound state problem is extremely hard as the coupling constant blows up at this point, and this makes perturbative calculations impossible. In 1979, three Russians, Shifman, Vainshstein and Zakharov (SVZ) [8] were the first to come up with the idea of approaching the bound state problem from the asymptotic freedom side. The method of QCD sum rules, first introduced by Shifman *et al.*, has become a popular and powerful technique to study hadronic physics in the low energy resonance region. As is well known, this method relates, through dispersion relations, low energy parameters, e.g. particle masses and coupling constants, to the

Operator Product Expansion (OPE) of current correlators at short distances. The basic underlying assumption is that this OPE remains valid in the presence of non-perturbative effects which are parameterized by a set of vacuum expectation values of quark and gluon fields. These vacuum condensates induce power corrections to asymptotic freedom and are supposed to be responsible for the rich resonance structure observed at low energies. To be more specific let us consider the following two-point function

$$\Pi\left(q^2\right) = i \int d^4x e^{iq\cdot x} \left\langle 0 | T\left(J\left(x\right) J^\dagger\left(0\right)\right) | 0 \right\rangle \tag{2.1}$$

where $J\left(x\right)$ stands for any local current built from the quark and gluon fields appearing in the QCD Lagrangian. The corresponding OPE reads

$$i \int d^4x e^{iq\cdot x} T\left(J\left(x\right) J^\dagger\left(0\right)\right) = C_0 \hat{1} + \sum_N C_N\left(q\right) \hat{O}_N \tag{2.2}$$

where the Wilson coefficients in this expansion depend on the Lorentz indices and quantum numbers of $J\left(x\right)$ and also the local gauge invariant operators $\hat{O}_N$ built from quark and gluon fields. These operators are ordered by increasing dimensionality and the Wilson coefficients, calculable in perturbation theory, fall off by corresponding powers of q^2. The unit operator in (2.2) has dimension $d = 0$ and $C_0\hat{1}$ stands for the purely perturbative contribution. Examples of $d = 4$ operators are $m_q\bar{q}q$ and $G^a_{\mu\nu}G^a_{\mu\nu}$. To use the OPE (2.2) in (2.1) one assumes that short and long distance effects factorize, the former are buried in the Wilson coefficients and the latter in the non-vanishing vacuum expectation values $\left\langle 0|\hat{O}_N|0\right\rangle$. After this, the rest follows from analiticity, viz. $\Pi\left(q^2\right)$ satisfies a dispersion relation and thus one relates the hadronic spectral function appearing there to the OPE. Different choices of the weight in the dispersion relation lead to different kinds of QCD sum rules, e.g. Hilbert, Laplace or Gaussian transforms, Finite energy Sum Rules (FESR), etc..

2.2 Types of sum rules

From Cauchy's theorem we obtain the dispersion relation

$$\Pi\left(Q^2\right) = \frac{1}{\pi}\int_0^\infty ds \frac{Im\Pi\left(s\right)}{s+Q^2} \quad + \quad subtractions \tag{2.3}$$

and spectral sum rules are merely different versions of the this dispersion relation, yielding in some cases an improvement. There are several well established sum rules of which each has its pros or cons depending on the application. The Laplace transform is extremely useful in the analysis of low-energy properties and is in fact the sum rule used in this thesis in order to extract the heavy-quark masses. Other sum rules such as the Moment sum rules are also good for the studying of low-energy properties of hadrons.

2.2.1 Moment Sum Rule

The moment sum rules are easily derived up to a multiplicative factor from the dispersion relation (2.3), by taking derivatives with respect to Q^2, i.e. the moment sum rule is

$$\mathcal{M}_n \equiv \frac{(-1)^n}{n!}\frac{d^n\Pi\left(Q^2\right)}{\left(dQ^2\right)^n} = \frac{1}{\pi}\int_0^\infty ds \frac{Im\Pi\left(s\right)}{\left(s+Q^2\right)^{n+1}}. \tag{2.4}$$

These sum rules were to our knowledge first discussed by Yndurain [9] in an attempt to study $e^+e^- \rightarrow$ *hadrons*. One needs to assume the existence of several derivatives of $\Pi\left(Q^2\right)$ in this sum rule. The moment sum rules (or power moments) are excellent for the study of low energy physics. For large (small) n, large (small) distances are probed. Starting with Q^2 large enough compared to the characteristic scale of confinement, one is in a regime where asymptotic freedom prevails. When n grows, the effect of confinement is probed due to forces coming into play in order to prevent the quarks from separating. Another important feature of the power moments is that as a result of taking various derivatives, one can eliminate subtraction terms in (2.3), which are often polynomials in Q^2.

experiment becomes a one parameter fit, the parameter being m_c (or m_b in the case of the beauty-quark). We find that the values of the (on-shell) masses from the fully relativistic ratios are in good agreement (within errors) with those from the non-relativistic ratios. We conclude with a comparison of our results with those obtained previously by other authors.

Since one is only considering heavy-quark systems, one can safely neglect operators with dimension $d > 4$, and thus apart from the identity operator, the only significant operator in heavy-quark systems is just the gluon condensate operator $G_a^{\mu\nu} G_{\mu\nu}^a$. This makes heavy-quark systems rather simple to analyze as one only has to calculate the Wilson coefficients for the identity operator and the operator $G_a^{\mu\nu} G_{\mu\nu}^a$.

One begins by considering the two-point function

$$\Pi(q) = i \int d^4x e^{iqx} \left\langle 0 \left| T\left(V_\mu(x) V_\nu^\dagger(0)\right|0\right)\right\rangle = \left(-g_{\mu\nu} q^2 + q_\mu q_\nu\right) \Pi\left(q^2\right) \tag{3.1}$$

with $V_\mu(x) = \bar{q}(x) \gamma_\mu q(x)$. This corresponds to the observed physical state $J^{PC} = 1^{--}$. The Wilson coefficients for all the possible currents that couple to observed physical states have been calculated by Reinders et al [12] , i.e. for the currents :

$$\begin{array}{ll} J_S^i = \bar{q}^i q^i & J^{PC} = 0^{++} \\ J_P^i = i\bar{q}^i \gamma_5 q^i & J^{PC} = 0^{--} \\ J_V^i = \bar{q}^i \gamma_\mu q^i & J^{PC} = 1^{--} \\ J_A^i = \eta_{\mu\nu} \bar{q}^i \gamma_\mu \gamma_5 q^i & J^{PC} = 1^{++} \\ J_A^{i\prime} = \bar{q}^i \overleftrightarrow{\partial}_\mu \gamma_5 q^i & J^{PC} = 1^{+-} \\ J_T^i = i\bar{q}^i \left(\gamma_\mu \overleftrightarrow{\partial}_\mu + \gamma_\nu \overleftrightarrow{\partial}_\mu + \frac{2}{3} \eta_{\mu\nu} \gamma_0 \overleftrightarrow{\partial}_\mu\right) q^i & J^{PC} = 2^{++} \end{array} \tag{3.2}$$

where $\eta_{\mu\nu} = q_\mu q_\nu / q^2 - g_{\mu\nu}$.

For our case of the vector current, the leading perturbative term in the Operator Product Expansion of $\Pi(q^2)$ involves calculating the Feynman diagrams

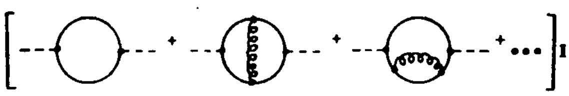

which has been calculated, by Schwinger, in perturbative QCD at the two-loop level [13], with its imaginary part given by his interpolation formula:

$$\frac{1}{\pi} Im\Pi(s)\,|_{QCD} = \frac{1}{8\pi^2} v\left(3 - v^2\right)\left\{1 + \frac{4\alpha_s}{3}\left[\frac{\pi}{2v} - \frac{(v+3)}{4}\left(\frac{\pi}{2} - \frac{3}{4\pi}\right)\right]\right\}\theta\left(s - 4m^2\right) \tag{3.3}$$

where $v = \sqrt{1 - 4m^2/s}$ and m is the quark on-shell mass : $m = m\left(Q^2 = m^2\right)$.

The leading non-perturbative term in the Operator Product Expansion of $\Pi(q^2)$ involves the gluon condensate, i.e.

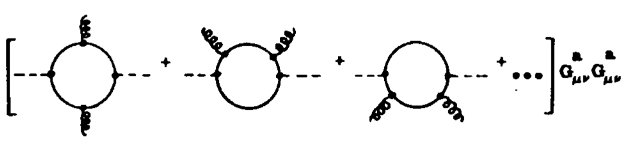

leading to the result

$$\Pi(s)\,|_{NP} = \frac{1}{48s^2}\left[\frac{3\left(v^2+1\right)\left(1-v^2\right)^2}{2v^5}\ln\frac{1+v}{1-v} - \frac{3v^4 - 2v^2 + 3}{v^4}\right]\left\langle\frac{\alpha_s}{\pi}G^2\right\rangle. \tag{3.4}$$

The function $\Pi(q^2)$ satisfies a once-subtracted dispersion relation, and the subtraction constant can be disposed of by taking the Laplace transform leaving one with the first Laplace moment. The relativistic and non-relativistic Laplace ratios are then defined by looking at the ratio of the first two Laplace moments, and from there the heavy-quark mass can be extracted.

3.2 Relativistic $\mathcal{R}(\sigma)$

It is preferable to use the moments

$$\mathcal{M}(\sigma) = \int ds \exp(-\sigma s) \, Im\Pi(s) \tag{3.5}$$

as the exponential weight cuts off large s contributions in $Im\Pi(s)$ more sharply than the power weight used by Reinders et al [12], and at relevant values of σ the ground state is the main contribution. The important difference is that the exponential factor increases the role of the ground state in the spectral integral if the variable σ is not too small. This is ideal for the case of low energy physics.

One can obtain the mass of the ground state by looking at the ratio of the moments, obtained from the logarithmic derivative of (3.5)

$$\mathcal{R}(\sigma) = -\frac{d}{d\sigma} \ln \mathcal{M}(\sigma) = -\frac{\mathcal{M}'(\sigma)}{\mathcal{M}(\sigma)}. \tag{3.6}$$

In the limit $\sigma \longrightarrow \infty$, $\mathcal{R}(\sigma)$ approaches the ground state mass. This can easily be seen by looking at the experimental side, where one parameterizes the experimental data by a sum of narrow resonances followed by a hadronic continuum modeled by perturbative QCD. In this case $\mathcal{M}(\sigma)$ is given by

$$\mathcal{M}(\sigma)|_{EXP} = \frac{3}{4\pi} \frac{1}{e_q^2 \alpha_{EM}^2} \sum_v \Gamma_v^{ee} M_v \exp\left(-\sigma M_v^2\right) + \frac{1}{\pi} \int_{s_0}^{\infty} ds \exp(-\sigma s) \, Im\Pi(s)|_{QCD} \tag{3.7}$$

where $Im\Pi(s)|_{QCD}$ is given by (3.3) and s_0 is the continuum threshold.

By doing a few simple manipulations it is a trivial matter to show that

$$\lim_{\sigma \to \infty} \mathcal{R}(\sigma) = M_{gr,st}^2 \tag{3.8}$$

using the expression for $\mathcal{M}(\sigma)$ in (3.7).

On the theoretical side we find that the ratio $\mathcal{R}(\sigma)$ has a minimum at finite σ and one regards this minimum as an approximation to the ground state

$$\min_{\sigma} \mathcal{R}(\sigma) = M^2_{gr,st}. \tag{3.9}$$

In [12], Reinders et al. worked with the moments

$$\mathcal{M}_n\left(Q^2\right) = \frac{1}{\pi}\int \frac{Im\Pi\left(s\right)}{\left(s+Q^2\right)^{n+1}}ds \tag{3.10}$$

and for convenience they wrote the power moments in the form

$$\mathcal{M}_n\left(Q^2\right) = A_n\left(Q^2\right)\left[1+\alpha_s a_n(Q^2)+\phi b_n\left(Q^2\right)\right] \tag{3.11}$$

where A_n is the free quark contribution, ϕ is the gluon condensate parameter, linked to the gluon condensate $\langle\alpha_s G^2\rangle$ by

$$\phi = \frac{\pi}{36}\frac{\langle\alpha_s G^2\rangle}{m^4}. \tag{3.12}$$

Also, the perturbative and non-perturbative contributions are separated and $\alpha_s a_n$ represents the first perturbative correction and ϕb_n represents the first non-perturbative correction.

Analogous to RRY and SVZ, Bertlmann [14] split the exponential moment (3.5) into the perturbative and non-perturbative parts in the following way

$$\mathcal{M}\left(\sigma\right) = \exp\left(-4m^2\sigma\right)\pi A\left(\sigma\right)\left[1+\alpha_s a\left(\sigma\right)+\phi b\left(\sigma\right)\right]. \tag{3.13}$$

Using the results of RRY, Bertlmann calculated the free quark term $\pi A\left(\sigma\right)$, the perturbative term $a\left(\sigma\right)$ and the non-perturbative term $b\left(\sigma\right)$. This was done by transforming (3.11) which was obtained using power moments to their corresponding counterpart, calculated by using the Laplace transform. Bertlmann further found that it was more convenient to work with the on-shell mass $m = m(p^2 = m^2)$. To obtain the mass of the heavy-quark, one works with the ratio of moments given in (3.13), and the ratio, rather than the moments, is perturbed. Using the ratio defined in (3.6), one obtains

$$\begin{aligned}
\mathcal{R}(\sigma) &= -\frac{d}{d\sigma}\ln\mathcal{M}(\sigma) \\
&= -\frac{d}{d\sigma}\left\{-4m^2\sigma+\ln\pi A(\sigma)\left[1+\alpha_s a(\sigma)+\phi b(\sigma)\right]\right\} \\
&= 4m^2-\frac{\pi A'(\sigma)}{\pi A(\sigma)}-\frac{\alpha_s a'(\sigma)+\phi b'(\sigma)}{1+\alpha_s a(\sigma)+\phi b(\sigma)}. \qquad (3.14)
\end{aligned}$$

It is important at this point to indicate a crucial difference between this result and Bertlmann's result [14] which is given by

$$\mathcal{R}(\sigma)=4m^2-\frac{d}{d\sigma}\left[\ln\pi A(\sigma)+\alpha_s a(\sigma)+\phi b(\sigma)\right]. \qquad (3.15)$$

Bertlmann has made the assumption that $\alpha_s a(\sigma)$ and $\phi b(\sigma)$ are sufficiently small to expand the denominator $(1+\alpha_s a(\sigma)+\phi b(\sigma))$ in (3.14), hence leading to his result given in (3.15). I have found that the first order corrections to the perturbative and non-perturbative terms are quite large and of $O(100\%)$, and thus this expansion of the denominator is unjustified and results in a higher estimate of the quark mass.

In calculating the ratio of the moments, it is more convenient to change variable. Letting $\omega=4m^2\sigma\Longrightarrow\frac{\partial}{\partial\sigma}=4m^2\frac{\partial}{\partial\omega}$ and performing the substitution, the ratio takes on the form

$$\mathcal{R}(\omega)=4m^2\left(1-\frac{\pi A'(\omega)}{\pi A(\omega)}-\frac{\alpha_s a'(\omega)+\phi b'(\omega)}{1+\alpha_s a(\omega)+\phi b(\omega)}\right) \qquad (3.16)$$

where the prime denotes the derivative with respect to ω. Putting all this together, one can proceed to calculate the free quark term $\pi A(\sigma)$, the perturbative term $\alpha_s a(\sigma)$ and the non-perturbative term $\phi b(\sigma)$ together with their derivatives to the next leading correction in $1/m^2$, and so obtain

$$\frac{\pi A'(\omega)}{\pi A(\omega)}=-\frac{1}{\omega}\left[\frac{3}{2}-\frac{5}{4}G\left(\tfrac{3}{2},\tfrac{7}{2},\omega\right)G^{-1}\left(\tfrac{1}{2},\tfrac{5}{2},\omega\right)\right] \qquad (3.17)$$

$$a(\omega)=\frac{4}{3\sqrt{\pi}}G^{-1}\left(\tfrac{1}{2},\tfrac{5}{2},\omega\right)\left[\pi-c_1G(1,2,\omega)+\frac{1}{3}c_2G(2,3,\omega)\right]-c_2 \qquad (3.18)$$

$$b(\omega) = -\frac{1}{2}\omega^2 G\left(-\tfrac{1}{2}, \tfrac{3}{2}, \omega\right) G^{-1}\left(\tfrac{1}{2}, \tfrac{5}{2}, \omega\right) \tag{3.19}$$

$$a'(\omega) = -\frac{4}{3\sqrt{\pi}} G^{-1}\left(\tfrac{1}{2}, \tfrac{5}{2}, \omega\right) \left\{ -c_1 G(2,2,\omega) + \frac{2}{3} c_2 G(3,3,\omega) - \frac{1}{2} G\left(\tfrac{3}{2}, \tfrac{5}{2}, \omega\right) \right.$$
$$\left. \times G^{-1}\left(\tfrac{1}{2}, \tfrac{5}{2}, \omega\right) \left[\pi - c_1 G(1,2,\omega) + \frac{1}{3} c_2 G(2,3,\omega) \right] \right\} \tag{3.20}$$

$$b'(\omega) = -\omega G^{-1}\left(\tfrac{1}{2}, \tfrac{5}{2}, \omega\right) \left\{ G\left(-\tfrac{1}{2}, \tfrac{3}{2}, \omega\right) + \frac{1}{4}\omega G\left(\tfrac{1}{2}, \tfrac{3}{2}, \omega\right) \right.$$
$$\left. + \frac{1}{4}\omega G\left(-\tfrac{1}{2}, \tfrac{3}{2}, \omega\right) G\left(\tfrac{3}{2}, \tfrac{5}{2}, \omega\right) G^{-1}\left(\tfrac{1}{2}, \tfrac{5}{2}, \omega\right) \right\} \tag{3.21}$$

where

$$c_1 = \frac{7\pi}{12} - \frac{3}{8\pi} \tag{3.22}$$

$$c_2 = \frac{\pi}{2} - \frac{3}{4\pi} \tag{3.23}$$

and $G(b, c, \omega)$ are Whittaker functions and are given by

$$G(b, c, \omega) = \frac{1}{\Gamma(c)} \int_0^\infty e^{-t} t^{c-1} (\omega + t)^{-b}\, dt. \tag{3.24}$$

They have nice derivative and asymptotic properties as well as satisfy several recurrence relations. All these properties can be found in Appendix A. The above expressions (3.17) - (3.21) involve no approximations, other than the two-loop perturbative expansion, and the leading non-perturbative term in the Operator Product Expansion. The expression (3.16) is referred to as the fully relativistic Laplace ratio.

Putting all these expressions together, one can rewrite the relativistic Laplace ratio in a more convenient form

$$\mathcal{R}(\sigma) = 4m^2 \left\{1 + \Delta_1 + f(\alpha_s \Delta_2 + \phi \Delta_3)\right\} \tag{3.25}$$

where

$$\Delta_1 = -\frac{\pi A'(\omega)}{\pi A(\omega)} \tag{3.26}$$

$$\Delta_2 = -a'(\omega) \tag{3.27}$$

$$\Delta_3 = -b'(\omega) \tag{3.28}$$

$$\Delta_4 = a(\omega) \tag{3.29}$$

$$\Delta_5 = b(\omega) \tag{3.30}$$

$$f = (1 + \alpha_s \Delta_4 + \phi \Delta_5)^{-1} \tag{3.31}$$

and the Δ_i are the perturbative and non-perturbative corrections, and f is a factor between $0-1$ due to the large perturbative and non-perturbative corrections. In Bertlmann's paper [14], these contributions were assumed to be negligible and this resulted in the absence of this factor f, that is to say in Bertlmann's paper the factor f is unity.

At this stage one is ready to compute the mass of the heavy-quark and the only input needed now is from the experimental side. One confronts (3.25) with a corresponding ratio involving the experimental data, which can obtained by taking the ratio of the moments given in (3.7). In this case the ratio is given by

$$\mathcal{R}(\sigma) = -\frac{d}{d\sigma} \ln \mathcal{M}(\sigma)\,|_{EXP}. \tag{3.32}$$

Using a computer program, one plots the theoretical and experimental ratios and determines the mass of the heavy-quark by varying the mass until the two curves agree. The agreement of the two curves will occur over some range of σ, centered about $\sigma_{\min}$ which is the minimum for the theoretical curve (3.25), and is regarded as an approximation to the square ground state mass as explained in (3.8). One hopes that $\sigma_{\min}$ is large enough so that (3.8) is valid. This is indeed found to be the case as one can see from the experimental curve which asymptotes very quickly.

The error in the mass comes from the uncertainty in the value of the gluon condensate $\langle \alpha_s G^2 \rangle$,

$$\langle \alpha_s G^2 \rangle = 0.063 - 0.19 \text{ GeV}^4 \tag{3.33}$$

and the value of Λ,

$$\Lambda_c = 200 - 300 \text{ MeV} \tag{3.34}$$

$$\Lambda_b = 100 - 200 \text{ MeV} \tag{3.35}$$

where Λ is the one fundamental constant of QCD that must be determined from experiment. Furthermore, it depends on the number of quark flavors, so it follows that when comparing Λ values, account must be taken of the number of quark flavors in each experiment. The results (3.34) - (3.35) were determined from results of the deep inelastic scattering experiment and the ratio of the hadronic to leptonic width of the Z experiment [15].

3.2.1 Behavior of $\mathcal{R}(\sigma)$

It is interesting to see the effect that Λ and the gluon condensate $\langle \alpha_s G^2 \rangle$ have on the ratio (3.25). In Fig. 3.2, one can see that the existence of a non-vanishing gluon condensate drives the theoretical curve (3.25) downwards, and in fact brings it closer to the ground state mass. For increasing σ, the curve deviates from experiment, and it is in fact the non-perturbative term which narrows the gap between experiment and theory. For $\sigma > \sigma_{\min}$, the approximation is no longer valid and in fact it breaks down.

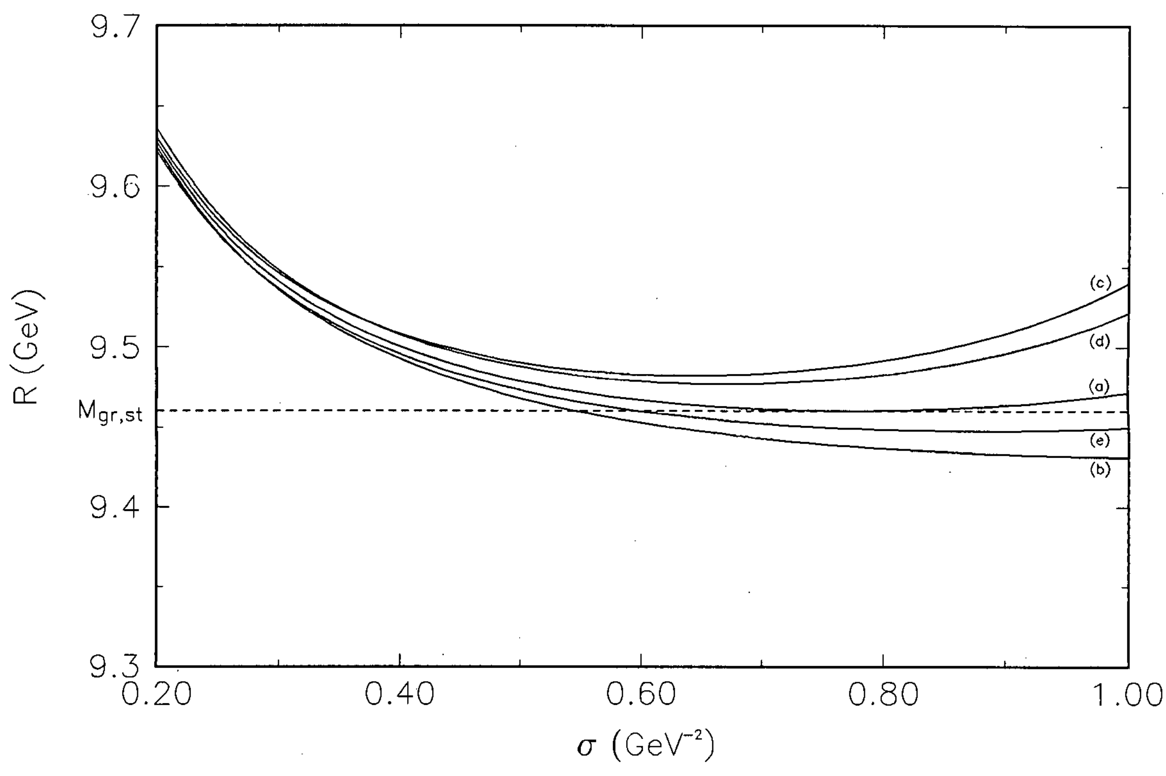

Figure 3.2: The behavior of the square root of theoretical ratio (3.25) for several choices of Λ and the gluon condensate value. Curve (a) is the reference curve. The remaining curves are achieved by decreasing the gluon condensate (curve (b)), increasing the gluon condensate (curve (c)), decreasing Λ (curve (d)) and increasing Λ (curve(e)).

In Fig. 3.2 , one can see that by increasing Λ, the minimum occurs for larger σ and this has the effect of increasing the value of the quark mass. On the other hand by increasing the value of the gluon condensate the opposite effect is achieved, and so to obtain the uncertainty in the quark mass, namely the upper and lower bounds, one needs to maximize Λ and minimize the gluon condensate to obtain the upper bound, and minimize Λ and maximize the gluon condensate to obtain the lower bound for the quark mass. This is done using the uncertainties given in (3.33) and (3.34) - (3.35).

One can also see from Fig. 3.3, that for large values of σ the gluon condensate contribution dominates.

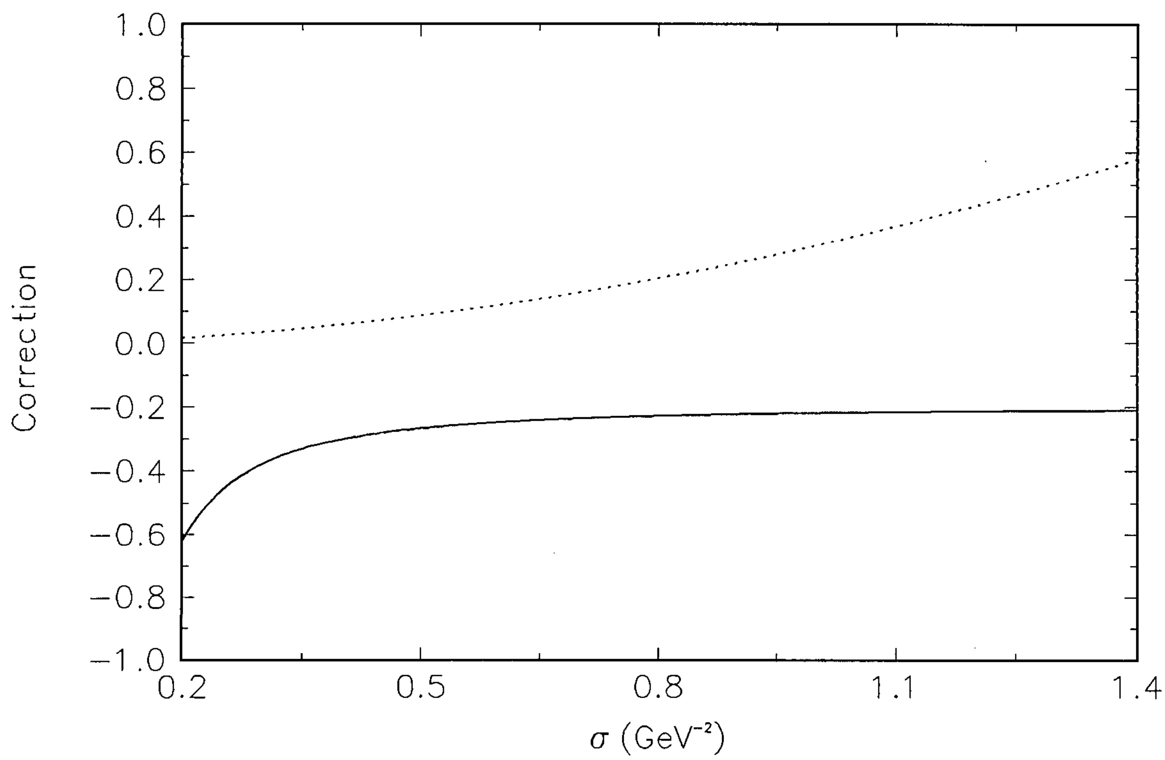

Figure 3.3: The perturbative correction $\alpha_s\Delta_2$ (solid curve) to the non-perturbative correction $\phi\Delta_3$ (dotted curve), for the case of the charm-quark.

3.2.2 The charm-quark mass m_c : relativistic determination

So far, I have derived an expression for the fully relativistic Laplace ratio of the moments $\mathcal{R}(\omega)$ as given in (3.16). Later on I shall derive an expression for the non-relativistic limit, and it will be shown that the charm is indeed heavy enough to be treated non-relativistically.

The charmonium system is quite different from the bottonium and toponium systems, as the charm-quark is much lighter than the bottom- and top-quarks. As a result, the charmonium system is not concentrated in a short range, like the heavier quark systems, where the coulomb force is strongly enhanced and confinement is severely suppressed. For this reason, the non-perturbative term containing the gluon condensate is far more important in the charmonium system than in the heavier quark systems.

The mass of the charm-quark is determined my matching the theoretical and experimental ratios around the minimum of (3.25). The theoretical ratio (3.25) exhibits a minimum around $\sigma \simeq 0.8 - 1.5\ \mathrm{GeV}^{-2}$, depending on the choice of Λ and the gluon condensate. The qualitative behavior of the square root of the experimental ratio (3.32) is a follows: At small σ, the ratio starts above the ground state mass and approaches it for increasing σ. For $\sigma \geq 0.8\ \mathrm{GeV}^{-2}$ it coincides with the mass of the J/ψ independently of the number of resonances included or the continuum threshold s_0, which is chosen at or below the $D\bar{D}$ threshold. Reasonable changes in the value of s_0 have essentially no impact on the results, hence, (3.13) is saturated mostly by the first two narrow resonances. For small values of σ, the $\psi(2S)$ and continuum represent a small correction.

In Table 3.1, I have computed the mass of the charm-quark for several options. One of the options is considering f set to unity so that a comparison can be made with Bertlmann's results in [14]. The correct situation is the former option and it is this choice for which the mass of the charm, m_c, is calculated, along with its error. The first and third combinations of values of Λ and the gluon condensate $\langle\alpha_s G^2\rangle$ in Table 3.1 were chosen so as to minimize and maximize the value of m_c. In Fig. 3.4, the theoretical and experimental curves are plotted for $\Lambda = 250$ MeV and $\langle\alpha_s G^2\rangle = 0.1265$ GeV^4, and $m_c = 1.42$ GeV. Changing the values of Λ and $\langle\alpha_s G^2\rangle$ leads to the result

$$m_c = 1.42 \pm 0.04 \text{ GeV}. \qquad (3.36)$$

In order to facilitate the comparison of (3.36) with previous determinations based on various versions of QCD sum rules [14], [16]- [21], we show in Fig. 3.5 the dependence of m_c on Λ for three different values of $\langle\alpha_s G^2\rangle$, and in Fig. 3.6 the dependence of m_c on the gluon condensate for Λ in the range: $\Lambda = 100 - 400$ MeV. Both figures correspond to the fully relativistic version of the QCD sum rules.

Λ	$\langle\alpha_s G^2\rangle$	Δ_1	$\alpha_s\Delta_2$	$\phi\Delta_3$	f	m_c
200	0.1900	0.230	-0.196	0.290	0.393	1.386
250	0.1265	0.177	-0.215	0.296	0.303	1.417
300	0.0630	0.114	-0.239	0.315	0.193	1.458
200	0.1900	0.315	-0.207	0.145	1	1.416
250	0.1265	0.264	-0.223	0.119	1	1.463
300	0.0630	0.196	-0.235	0.090	1	1.524

Table 3.1: Relativistic results for the charm-quark.

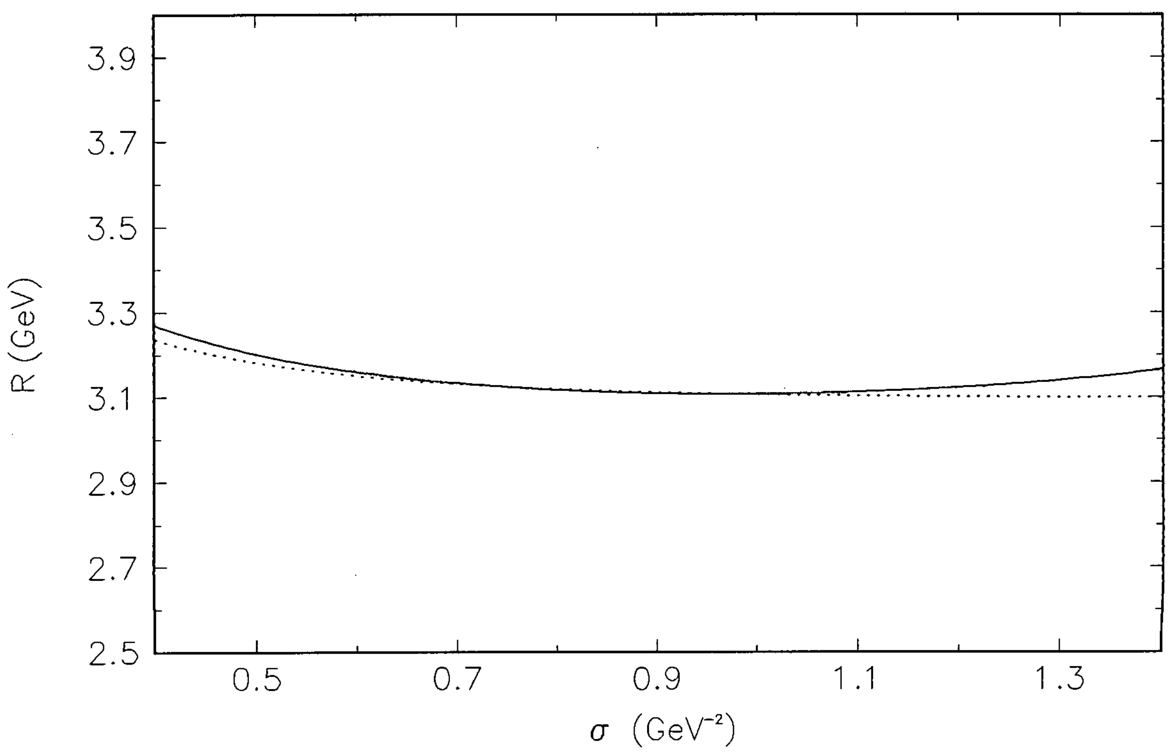

Figure 3.4: The square-root of the fully relativistic ratio (3.25) (solid curve), and the experimental ratio (3.32) (broken curve). The values of the parameters are: $\Lambda = 250$ MeV, $\langle \alpha_s G^2 \rangle = 0.1265$ GeV^4, and $m_c = 1.42$ GeV.

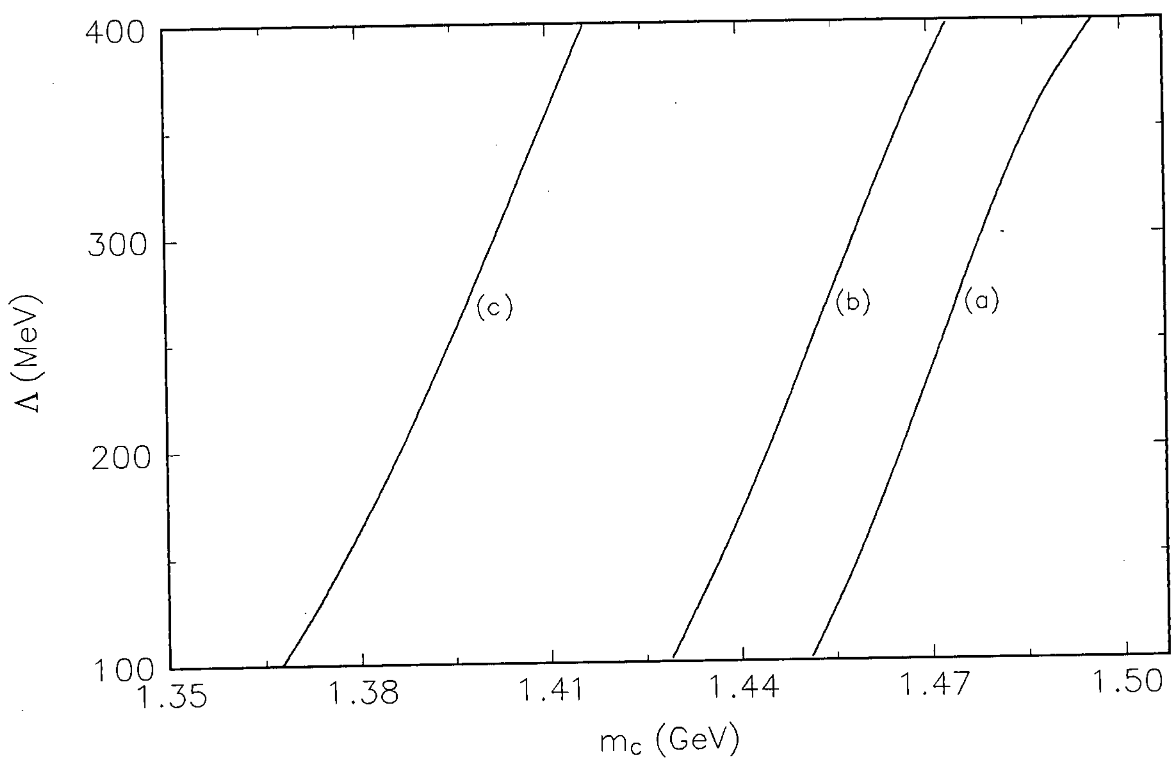

Figure 3.5: Dependence of m_c on Λ for $\langle \alpha_s G^2 \rangle = 0.038$ GeV^4 (curve (a)), 0.063 GeV^4 (curve (b)), and 0.19 GeV^4 (curve (c)). The fully relativistic ratio (3.25) has been used. Curve (a) is shown for reference purposes, as this low value of $\langle \alpha_s G^2 \rangle$ was not used in our analysis.

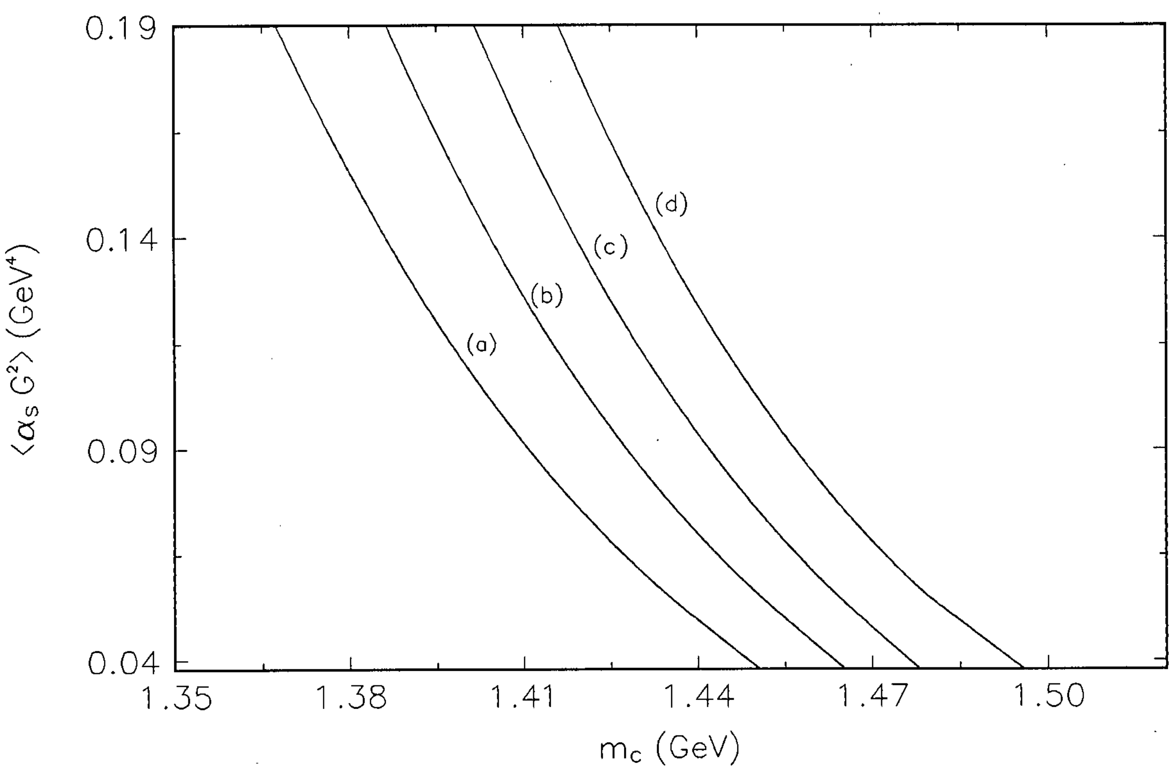

Figure 3.6: Dependence of m_c on $\langle \alpha_s G^2 \rangle$ for Λ = 100 MeV (curve (a)), 200 MeV (curve (b)), 300 MeV (curve (c)), and 400 MeV (curve (d)). The fully relativistic ratio (3.25) has been used. Curves (a) and (d) are shown for reference purposes, as these extreme values of Λ were not used in our analysis.

3.2.3 The beauty-quark mass m_b : relativistic determination

The mass of the beauty-quark is determined my matching the theoretical and experimental ratios around the minimum of (3.25). The theoretical ratio (3.25) exhibits a minimum around $\sigma \simeq 0.4 - 0.8$ GeV^{-2}, depending on the choice of Λ and the gluon condensate. The qualitative behavior of the square root of the experimental ratio (3.32) is a follows. At small σ, the ratio starts above the ground state mass and approaches it for increasing σ. For $\sigma \geq 0.4$ GeV^{-2} it coincides with the mass of the Υ(1S) independently of the number of resonances included or the onset of the continuum. For small values of σ, the Υ(2S), Υ (3S) and the continuum represent a small correction.

In Table 3.2, I have computed the mass of the beauty-quark for several options. One of the options is considering f set to unity so that a comparison can be made with Bertlmann's results in [14]. The correct situation is the former option and it is this choice for which the mass of the beauty, m_b, is calculated, along with its error. The two combinations of values of Λ and the gluon condensate $\langle \alpha_s G^2 \rangle$ were chosen so as to minimize and maximize the value of m_b. In Fig.3.7, the theoretical and experimental curves are plotted for Λ = 150 MeV and $\langle \alpha_s G^2 \rangle$ = 0.1265 GeV^4 and m_b = 4.65 GeV. Changing the values of Λ and $\langle \alpha_s G^2 \rangle$ leads to the result

$$m_b = 4.65 \pm 0.02 \text{ GeV}. \tag{3.37}$$

In order to facilitate the comparison of (3.37) with previous determinations based on various versions of QCD sum rules [14], [16]- [21], we show in Fig. 3.8 the dependence of m_b on Λ for three different values of $\langle \alpha_s G^2 \rangle$, and in Fig. 3.9 the dependence of m_b on the gluon condensate for Λ in the range: $\Lambda = 100 - 400$ MeV. Both figures correspond to the fully relativistic version of the QCD sum rules.

Λ	$\langle \alpha_s G^2 \rangle$	Δ_1	$\alpha_s \Delta_2$	$\phi \Delta_3$	f	m_b
100	0.1900	0.040	-0.058	0.074	0.247	4.630
150	0.1265	0.032	-0.063	0.079	0.187	4.651
200	0.0630	0.022	-0.067	0.081	0.128	4.675
100	0.1900	0.069	-0.068	0.024	1	4.686
150	0.1265	0.060	-0.075	0.020	1	4.727
200	0.0630	0.049	-0.080	0.015	1	4.774

Table 3.2: Relativistic results for the beauty-quark.

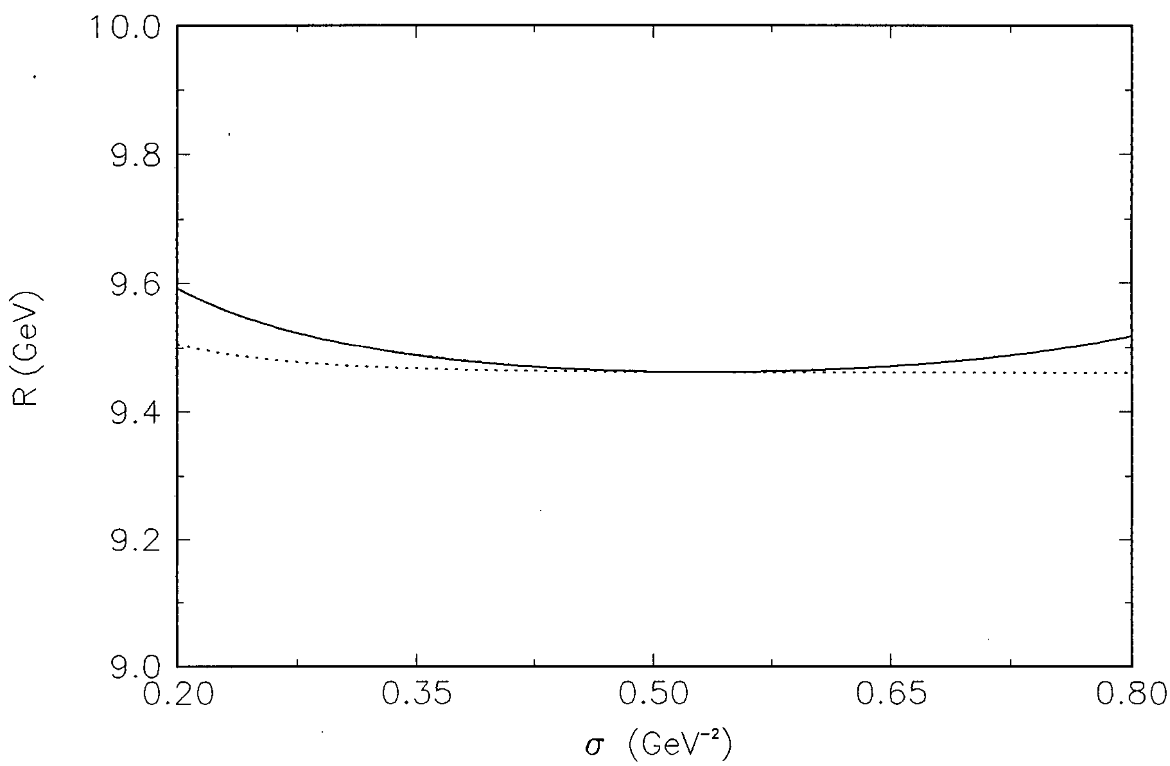

Figure 3.7: The square-root of the fully relativistic ratio (3.25) (solid curve), and the experimental ratio (3.32) (broken curve). The values of the parameters are: $\Lambda = 150$ MeV, $\langle \alpha_s G^2 \rangle = 0.1265$ GeV^4, and $m_b = 4.65$ GeV.

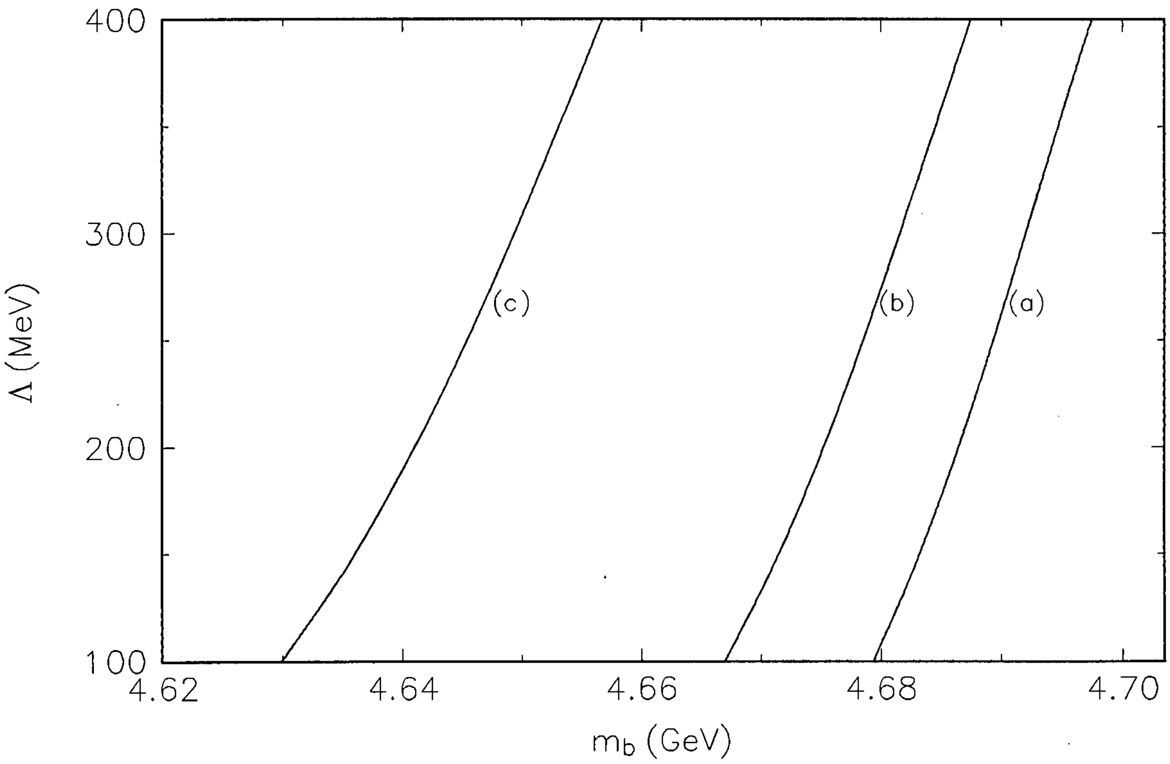

Figure 3.8: Dependence of m_b on Λ for $\langle \alpha_s G^2 \rangle = 0.038$ GeV^4 (curve (a)), 0.063 GeV^4 (curve (b)), and 0.19 GeV^4 (curve (c)). The fully relativistic ratio (3.25) has been used. Curve (a) is shown for reference purposes, as this low value of $\langle \alpha_s G^2 \rangle$ was not used in our analysis.

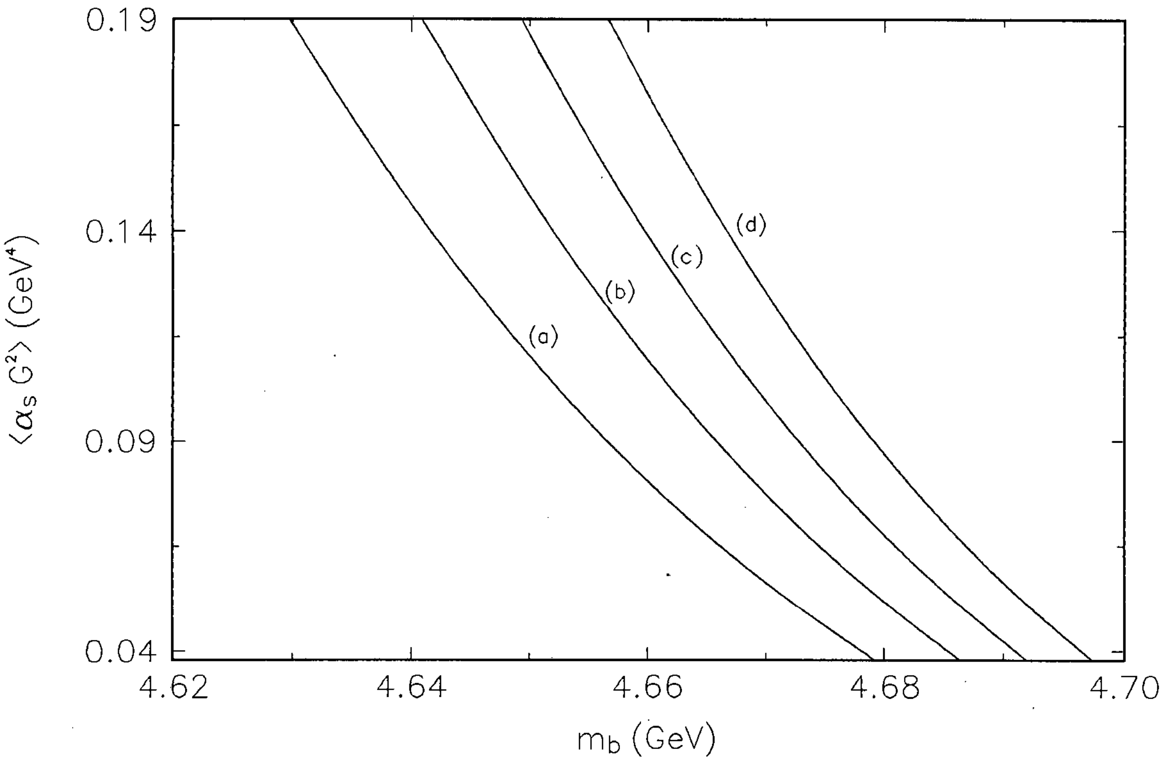

Figure 3.9: Dependence of m_b on $\langle \alpha_s G^2 \rangle$ for Λ = 100 MeV (curve (a)), 200 MeV (curve (b)), 300 MeV (curve (c)), and 400 MeV (curve (d)). The fully relativistic ratio (3.25) has been used. Curves (c) and (d) are shown for reference purposes, as these extreme values of Λ were not used in our analysis.

3.3 Non-relativistic $\mathcal{R}(\tau)$

The non-relativistic limit is achieved by assuming the infinite mass limit. Writing

$$s = (2m + E)^2 \tag{3.38}$$

and neglecting terms of $O(E^2)$, the relativistic moment (3.5) becomes

$$\begin{aligned} \mathcal{M}(\sigma) &= \int \exp(-\sigma s)\, Im\Pi(s)\, ds \\ &\approx \int \exp\left(-4\sigma m^2 - 4mE\sigma\right) 2(2m+E) Im\Pi(E)\, dE \\ &\approx \exp\left(-4m^2\sigma\right) 4m \int \exp(-4m\sigma E)\, Im\Pi(E)\, dE \\ &= 4me^{-m\tau}\mathcal{M}(\tau) \end{aligned} \tag{3.39}$$

with $\tau = 4m\sigma$, and

$$\mathcal{M}(\tau) = \int dE e^{-\tau E} Im\Pi(E). \tag{3.40}$$

The non-relativistic ratio is defined as

$$\mathcal{R}(\tau) = 2m - \frac{d}{d\tau}\ln \mathcal{M}(\tau). \tag{3.41}$$

There is a link between the relativistic ratio (3.6) and the non-relativistic ratio (3.41), namely

$$\begin{aligned} \mathcal{R}(\tau) &= -\frac{d}{d\tau}\ln \mathcal{M}(\tau) \\ &= 2m - \frac{d}{d\tau}\ln\left\{\frac{\exp\left(4m^2\sigma\right)}{4m}\mathcal{M}(\sigma)\right\} \\ &= 2m - \frac{d}{d(4m\sigma)}\left\{\ln \mathcal{M}(\sigma) - \ln(4m) + 4m^2\sigma\right\} \\ &= 2m + \frac{1}{4m}\left\{\mathcal{R}(\sigma) - 4m^2\right\}. \end{aligned} \tag{3.42}$$

Now recall (3.9), so if one writes $M_{gr,st} = 2m + \Delta$ then at $\sigma_{\min}$ one has

$$\mathcal{R}(\tau) = 2m + \frac{1}{4m}\left\{4m^2 + 4m\Delta + \Delta^2 - 4m^2\right\} = 2m + \Delta + \frac{\Delta^2}{4m} \tag{3.43}$$

so (3.41) is approximately the ground state mass. Hence, one obtains a direct link with the square root of the non-relativistic ratio (3.6), namely

$$\mathcal{R}(\tau) = \sqrt{\mathcal{R}(\sigma)} = M_{gr,st}. \tag{3.44}$$

Substituting $\mathcal{R}(\sigma)$ given in (3.25) one obtains the non-relativistic ratio

$$\mathcal{R}(\tau) = 2m\left\{1 + \frac{1}{2}\Delta_1 + \frac{1}{2}f\left(\alpha_s\Delta_2 + \phi\Delta_3\right)\right\} \tag{3.45}$$

where Δ_i are given in (3.26) - (3.30) and f is given in (3.31). Now the non-relativistic ratio was derived in the infinite mass limit and it would thus be sensible to expand $\mathcal{R}(\tau)$ in powers of $1/m$. In this way one can see where the expression breaks down (i.e. where higher order corrections are of $O(100\%)$) and thus determine if the quark is heavy enough to be treated non-relativistically or not.

Using the approximation to the Whittaker functions, and expanding the Δ_i given in (3.26 - 3.30) in powers of $1/m$ (a small value) one gets

$$\Delta_1 = \frac{3}{2m\tau}\left(1 - \frac{5}{6}\frac{1}{m\tau} + \frac{10}{3}\frac{1}{m^2\tau^2}\right) \tag{3.46}$$

$$\Delta_2 = -\frac{2\sqrt{\pi}}{3}\frac{1}{\sqrt{m\tau}}\left[1 - \left(\frac{2}{3} + \frac{3}{8\pi^2}\right)\frac{1}{m\tau} + \frac{1}{32}\left(107 + \frac{51}{\pi^2}\right)\frac{1}{m^2\tau^2}\right] \tag{3.47}$$

$$\Delta_3 = \frac{3}{2}\frac{1}{m^2\tau^2}\left(1 + \frac{4}{3}\frac{1}{m\tau} - \frac{5}{12}\frac{1}{m^2\tau^2}\right) \tag{3.48}$$

$$\Delta_4 = \frac{4\sqrt{\pi}}{3}\sqrt{m\tau}\left[1 + \left(\frac{2}{3} + \frac{3}{8\pi^2}\right)\frac{1}{m\tau} - \frac{1}{32}\left(\frac{107}{3} + \frac{17}{\pi^2}\right)\frac{1}{m^2\tau^2}\right] \tag{3.49}$$

$$\Delta_5 = -\frac{1}{2}\frac{1}{m^3\tau^3}\left(1 + \frac{2}{m\tau} - \frac{5}{4}\frac{1}{m^2\tau^2}\right) \tag{3.50}$$

and the non-relativistic Laplace ratio is

$$\mathcal{R}(\tau) = 2m\left\{1 + \frac{3}{4m\tau}\left(1 - \frac{5}{6}\frac{1}{m\tau} + \frac{10}{3}\frac{1}{m^2\tau^2}\right)\right.$$
$$- \frac{\sqrt{\pi}}{3}\frac{\alpha_s}{\sqrt{m\tau}}\left[1 - \left(\frac{2}{3} + \frac{3}{8\pi^2}\right)\frac{1}{m\tau} + \frac{1}{32}\left(107 + \frac{51}{\pi^2}\right)\frac{1}{m^2\tau^2}\right]$$
$$\left. + \frac{\pi}{48}\frac{\tau^2}{m^2}\left\langle\alpha_s G^2\right\rangle\left(1 + \frac{4}{3}\frac{1}{m\tau} - \frac{5}{12}\frac{1}{m^2\tau^2}\right)\right\} \tag{3.51}$$

where in this definition we have set f to unity. The justification for this comes from the very important fact that the expanded[1] non-relativistic ratio is invariant under changes of the quark mass definition [22]. Although, for the case of the on-shell quark mass, the factor f was found to differ significantly from unity, due to the large perturbative and non-perturbative corrections, one could in principle use a different quark mass definition,[2] the off-shell mass $\tilde{m} = \tilde{m}\left(p^2 = -\tilde{m}^2\right)$ which differs from the on-shell mass m through an α_s correction

$$m = \tilde{m} + \delta\tilde{m} \tag{3.52}$$

where

$$\delta\tilde{m} = \alpha_s\frac{2\ln 2}{\pi}\tilde{m} \tag{3.53}$$

thereby bringing f nearer to unity and thus making it possible to expand. Expanding f one can then show that

$$\tilde{\mathcal{R}}(\tau) = 2\tilde{m} - \frac{d}{d\tau}\ln\tilde{\mathcal{M}}(\tau) = 2m - \frac{d}{d\tau}\ln\mathcal{M}(\tau) = \mathcal{R}(\tau) \tag{3.54}$$

hereby showing its invariance under the quark mass definition. One can always find such a quark mass definition which diminishes the $\alpha_s\Delta_4$ and $\phi\Delta_5$ corrections to the moment, allowing one to set f to unity. We may thus work with the ratio (3.51). Working with the non-expanded form leaves one with no clear distinction between the relativistic and non-relativistic Laplace ratios, and furthermore it does not allow one to obtain $\mathcal{R}(\tau)$ as an expansion in $1/m$ which is needed for the infinite mass limit to make sense.

[1] By expanded, we mean expanding f in powers of $1/m$.
[2] Introduced by the ITEP group [20].

3.3.1 The charm-quark mass m_c : non-relativistic determination

Unlike the beauty- or the top-quark, which are clearly heavy enough to be considered non-relativistically, whether or not the charm-quark is heavy enough to be treated non-relativistically is still an open question. Recently, the value of the (on-shell) beauty-quark mass has been determined [23] by confronting very accurate experimental data on the upsilon system [15] with ratios of non-relativistic Laplace transform QCD moments. This theoretical framework, suggested by Bertlmann [14], offers several advantages, e.g. radiative and non-perturbative corrections are well under control, and the non-relativistic limit follows quite naturally from quantum mechanical analogues [24]. This version of QCD sum rules leads to an expansion in powers of the inverse of the heavy-quark mass which allows one to test the range of validity of the non-relativistic limit, and more generally, to assess the role of mass corrections. This might be of interest for calculations based on the simplifying assumption $\Lambda_{QCD}/m_Q \ll 1$.

Non-relativistic Laplace moments appear to have a sensitive dependence on the quark mass. In fact, in spite of the large uncertainties affecting the values of Λ_{QCD} and the non-perturbative gluon condensate, m_b can be extracted from the upsilon data with high precision. This extraction is performed by confronting the ratios of Laplace transform moments calculated from experiment with those from theory. The latter involve the QCD parameters m_b, Λ, $\langle \alpha_s G^2 \rangle$, etc.. These ratios are functions of the Laplace variable, which acts as a short distance expansion parameter, and one finds a reasonably wide region in this variable where there is a matching between experiment and theory for a specific value of the quark mass.

As pointed out in [23], a straightforward extension of this technique to the charm-quark may not work, as radiative and mass corrections could exceed 100%. This would be true if the window in the Laplace variable would be the same for beauty and for charm. However, there is no *a-priori* reason for this to be the case. In fact, as also suggested in [14], the matching between theory and experiment for the beauty- and the charm-quarks could take place at different ranges of the Laplace variable. If this range is such that radiative, non-perturbative, and mass corrections remain small, then it would become possible to extract the value of the charm-quark from this framework. Thus it is of great importance to finally settle this question. Using the non-relativistic ratio (3.51), and looking at the size of the next-to-leading corrections in powers of $1/m$, it will be shown that the charm-quark is indeed heavy enough to be treated non-relativistically. At least in this application.

The mass of the charm is determined my matching the theoretical and experimental ratios around the minimum of the theoretical ratio (3.25). The theoretical ratio (3.25) exhibits a minimum around $\sigma \simeq 0.6 - 0.8$ GeV^{-2}, depending on the choice of Λ and the gluon condensate. Over this range of σ, the sub-leading quark mass corrections are of a few percent and are thus at a very safe level. The qualitative behavior of the square root of the experimental ratio (3.32) is the same as for the relativistic determination, except that for $\sigma \geq 0.6$ GeV^{-2} it coincides with the mass of the J/ψ independently of the number of resonances included or the continuum threshold s_0.

The first and third combinations of values for Λ and the gluon condensate $\langle \alpha_s G^2 \rangle$ in Table 3.3, were chosen so as to minimize and maximize the value of m_c. In Fig. 3.10, the theoretical and experimental curves are plotted for $\Lambda = 250$ MeV and $\langle \alpha_s G^2 \rangle = 0.1265$ GeV^4 and $m_c = 1.45$ GeV. Changing the values of Λ and $\langle \alpha_s G^2 \rangle$ leads to the result

$$m_c = 1.46 \pm 0.07 \text{ GeV}. \tag{3.55}$$

In order to facilitate the comparison of (3.55) with previous determinations based on various versions of QCD sum rules [14], [16] - [21], we show in Fig. 3.11 the dependence of m_c on Λ for three different values of $\langle \alpha_s G^2 \rangle$, and in Fig. 3.12 the dependence of m_c on the gluon condensate for Λ in the range: $\Lambda = 100 - 400$ MeV. Both figures correspond to the non-relativistic version of the QCD sum rules.

Λ	$\langle \alpha_s G^2 \rangle$	Δ_1	$\alpha_s \Delta_2$	$\phi \Delta_3$	m_c
200	0.1900	0.334	-0.229	0.166	1.390
250	0.1265	0.275	-0.237	0.126	1.454
300	0.0630	0.201	-0.247	0.090	1.525

Table 3.3: non-Relativistic results for the charm-quark.

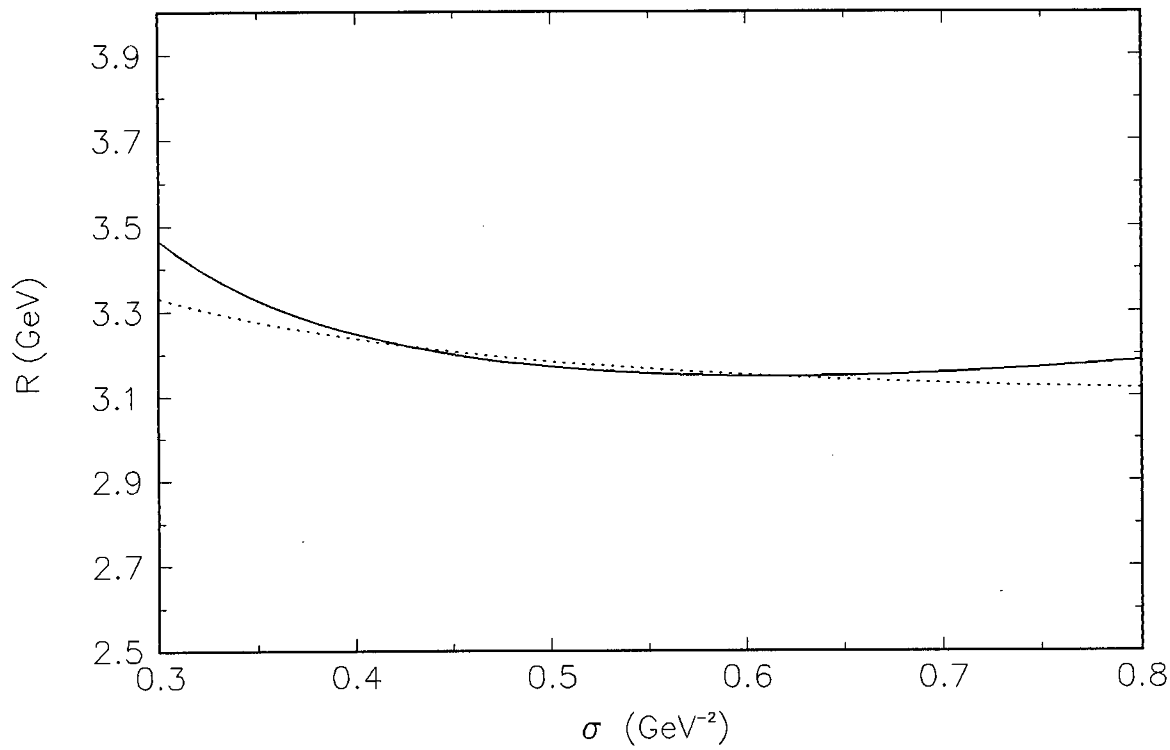

Figure 3.10: The non-relativistic ratio (3.51) (solid curve), and and the square-root of the experimental ratio (3.32) (broken curve). The values of the parameters are: $\Lambda = 250$ MeV, $\langle \alpha_s G^2 \rangle = 0.1265$ GeV^4, and $m_c = 1.45$ GeV.

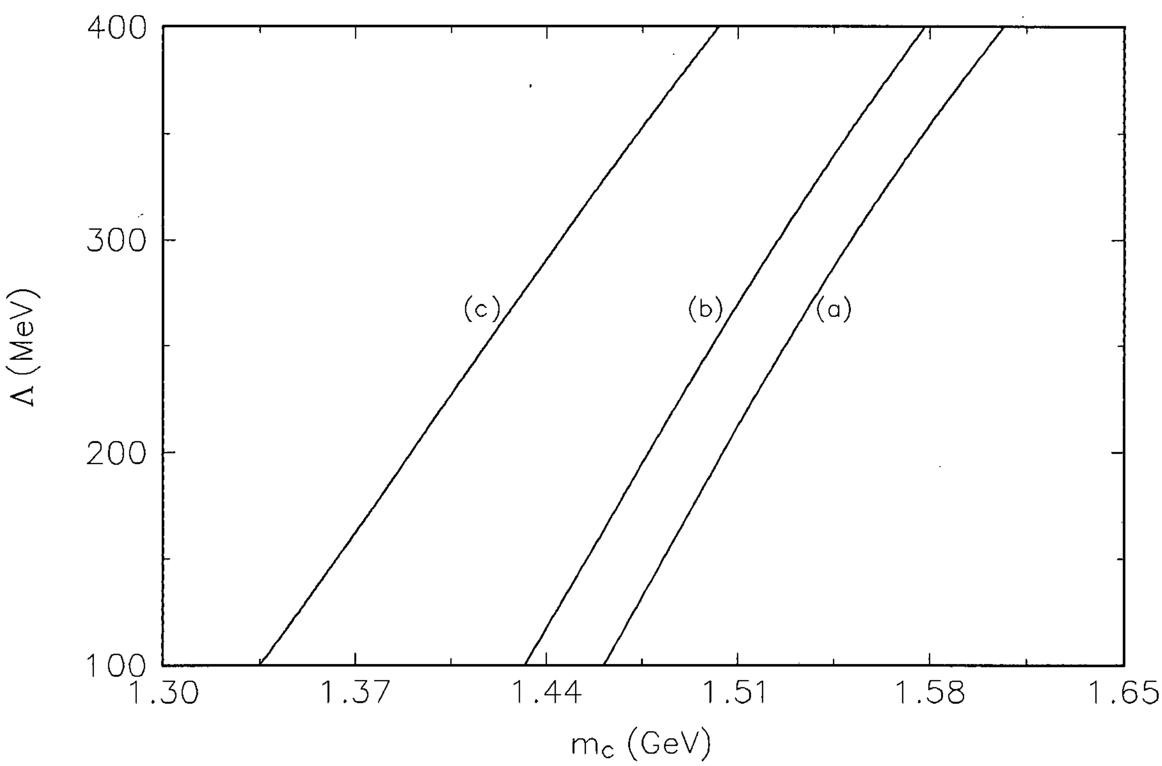

Figure 3.11: Dependence of m_c on Λ for $\langle \alpha_s G^2 \rangle = 0.038$ GeV^4 (curve (a)), 0.063 GeV^4 (curve (b)), and 0.19 GeV^4 (curve (c)). The non-relativistic ratio (3.51) has been used. Curve (a) is shown for reference purposes, as this low value of $\langle \alpha_s G^2 \rangle$ was not used in our analysis.

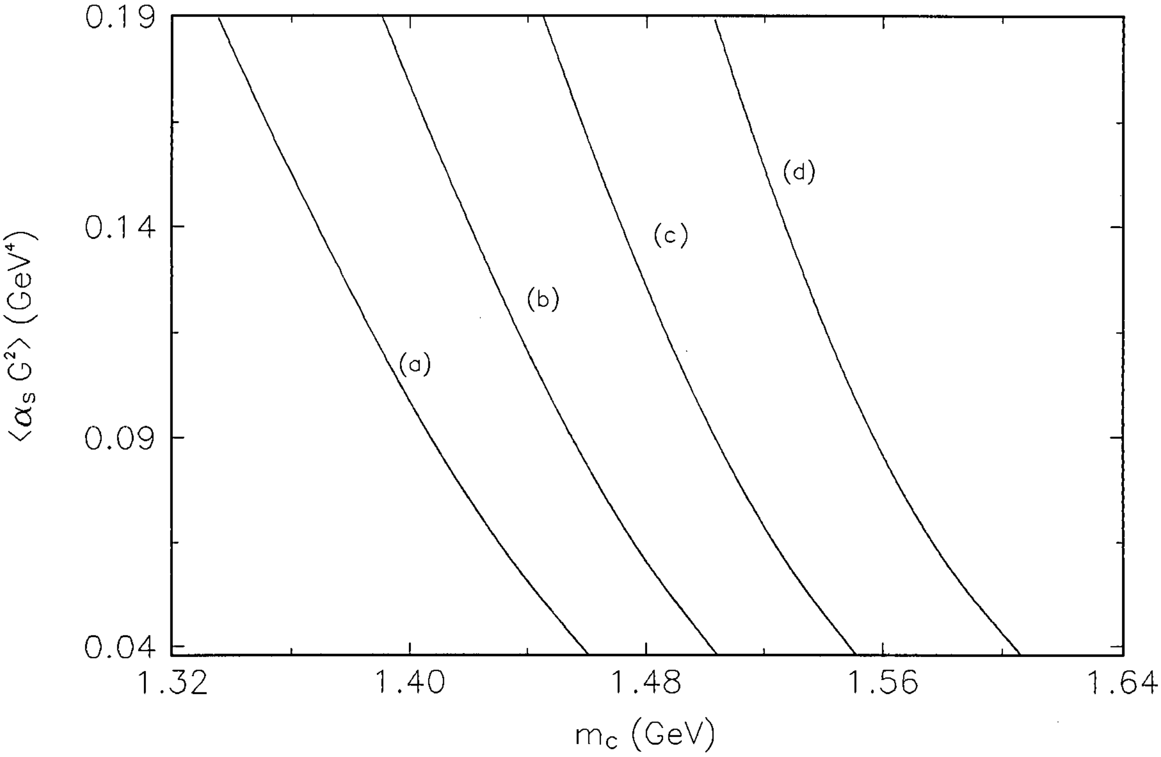

Figure 3.12: Dependence of m_c on $\langle \alpha_s G^2 \rangle$ for Λ = 100 MeV (curve (a)), 200 MeV (curve (b)), 300 MeV (curve (c)), and 400 MeV (curve (d)). The non-relativistic ratio (3.51) has been used. Curves (a) and (d) are shown for reference purposes, as these extreme values of Λ were not used in our analysis.

3.3.2 The beauty-quark mass m_b : non-relativistic determination

The mass of the beauty is determined my matching the theoretical and experimental ratios around the minimum of the theoretical ratio (3.51). The theoretical ratio (3.51) exhibits a minimum around $\sigma \simeq 0.2 - 0.3$ GeV^{-2}, depending on the choice of Λ and the gluon condensate. The qualitative behavior of the square root of the experimental ratio (3.32) is the same as in the relativistic determination, except that for $\sigma \geq 0.2$ GeV^{-2} it coincides with the mass of the Υ (1S) independently of the number of resonances included or the start of the continuum.

In Table 3.4, I have computed the mass of the beauty-quark for several options. The two combinations of values for Λ and the gluon condensate $\langle \alpha_s G^2 \rangle$ were chosen so as to minimize and maximize the value of m_b. In Fig. 3.13, the theoretical and experimental curves are plotted for $\Lambda = 150$ MeV and $\langle \alpha_s G^2 \rangle = 0.1265$ GeV^4 and $m_b = 4.72$ GeV. Changing the values of Λ and $\langle \alpha_s G^2 \rangle$ leads to the result

$$m_b = 4.73 \pm 0.04 \text{ GeV}. \tag{3.56}$$

In order to facilitate the comparison of (3.56) with previous determinations based on various versions of QCD sum rules [14], [16] - [21], we show in Fig. 3.14 the dependence of m_b on Λ for three different values of $\langle \alpha_s G^2 \rangle$, and in Fig. 3.15 the dependence of m_b on the gluon condensate for Λ in the range: $\Lambda = 100 - 400$ MeV. Both figures correspond to the non-relativistic version of the QCD sum rules.

Λ	$\langle\alpha_s G^2\rangle$	Δ_1	$\alpha_s\Delta_2$	$\phi\Delta_3$	m_b
100	0.1900	0.069	-0.068	0.024	4.685
150	0.1265	0.060	-0.075	0.020	4.727
200	0.0630	0.049	-0.080	0.015	4.774

Table 3.4: non-Relativistic results for the beauty-quark.

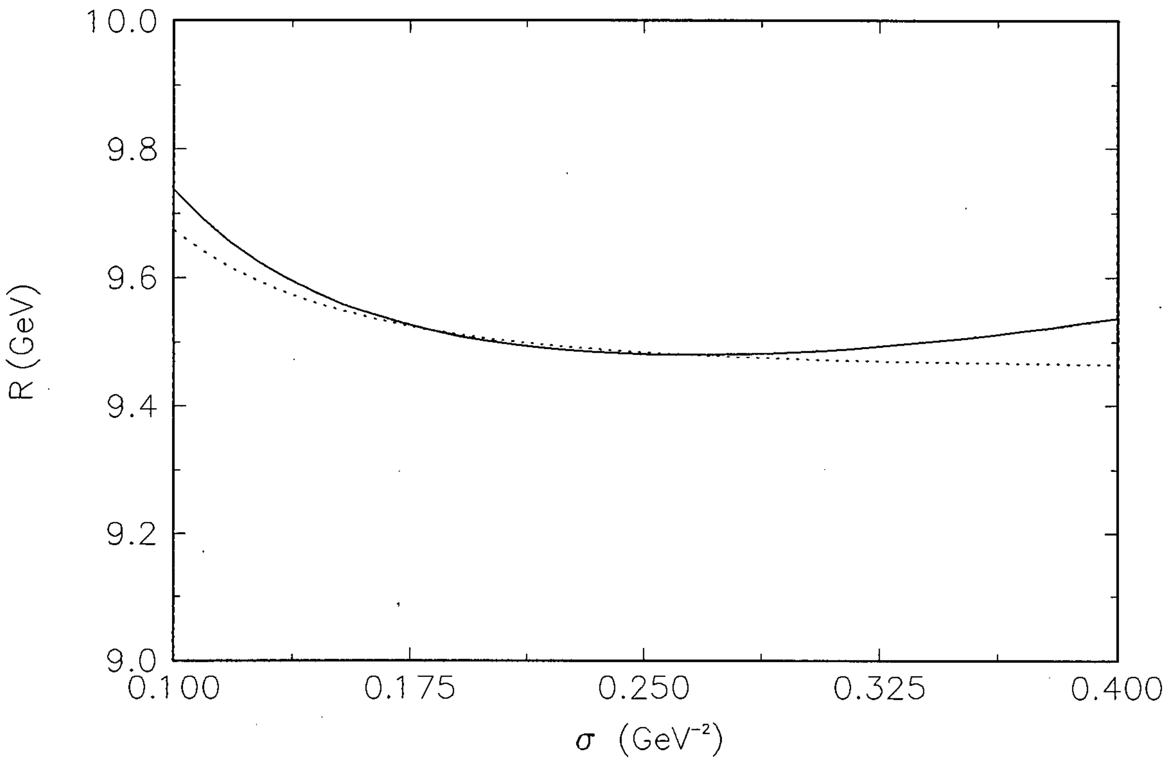

Figure 3.13: The non-relativistic ratio (3.51) (solid curve), and the square-root of the experimental ratio (3.32) (broken curve). The values of the parameters are: $\Lambda = 150$ MeV, $\langle\alpha_s G^2\rangle = 0.1265$ GeV^4, and $m_b = 4.72$ GeV.

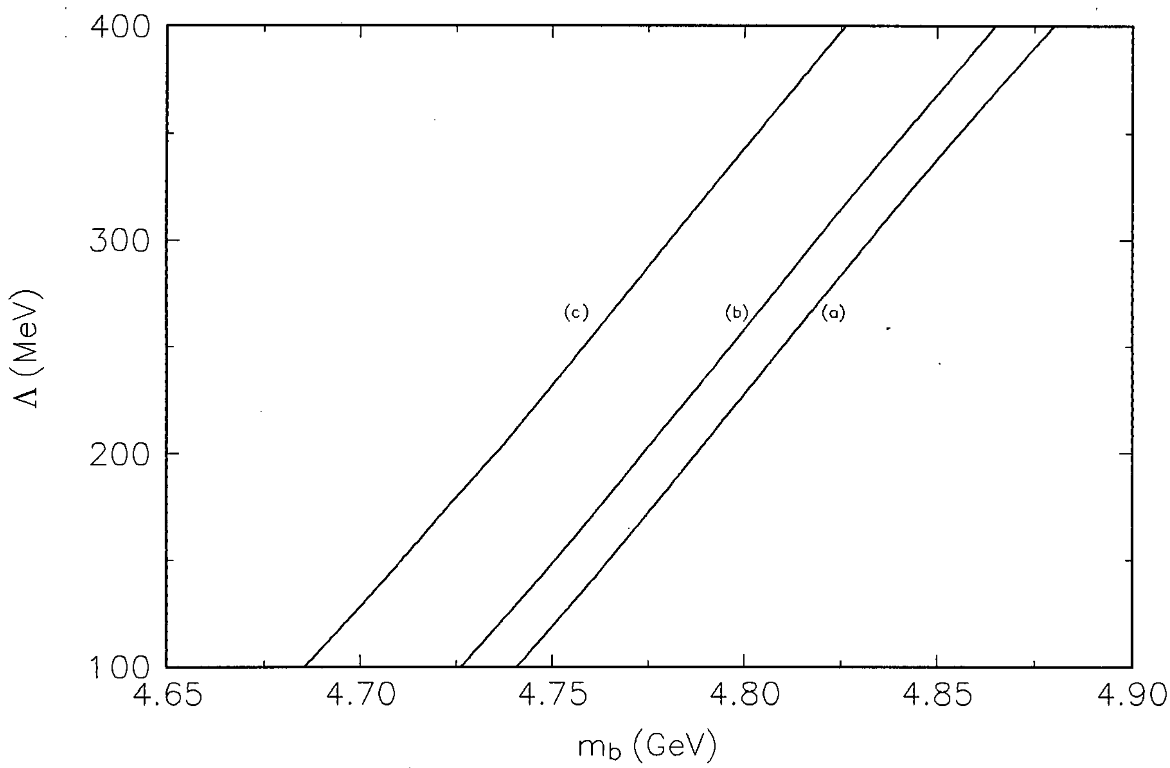

Figure 3.14: Dependence of m_b on Λ for $\langle \alpha_s G^2 \rangle = 0.038\ \mathrm{GeV}^4$ (curve (a)), $0.063\ \mathrm{GeV}^4$ (curve (b)), and $0.19\ \mathrm{GeV}^4$ (curve (c)). The non-relativistic ratio (3.51) has been used. Curve (a) is shown for reference purposes, as this low value of $\langle \alpha_s G^2 \rangle$ was not used in our analysis.

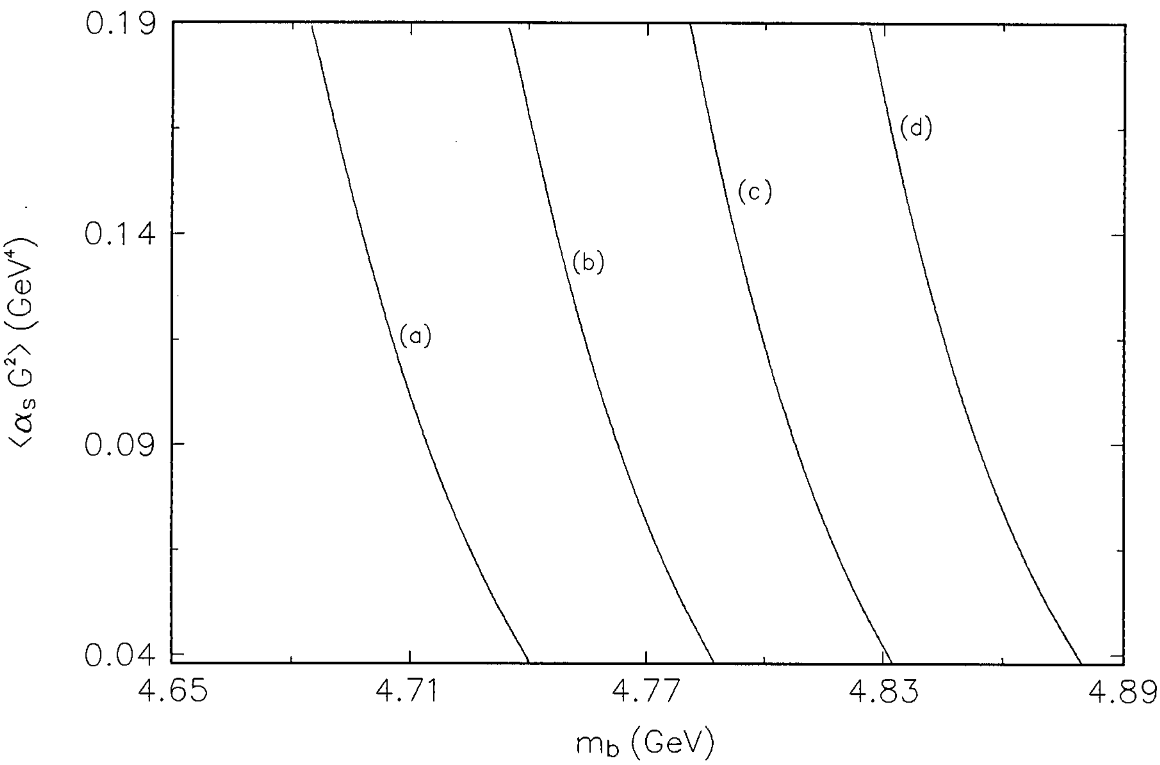

Figure 3.15: Dependence of m_b on $\langle \alpha_s G^2 \rangle$ for Λ = 100 MeV (curve (a)), 200 MeV (curve (b)), 300 MeV (curve (c)), and 400 MeV (curve (d)). The non-relativistic ratio (3.51) has been used. Curves (c) and (d) are shown for reference purposes, as these extreme values of Λ were not used in our analysis.

3.4 Effect of α_s correction to $\langle\alpha_s G^2\rangle$

Recently [25], the two-loop correction to the Wilson coefficient of the gluon condensate has been calculated. We have incorporated this additional term in the Laplace ratios, and find that the correction it introduces is about a factor of 2 larger than the $1/m_c$ correction to $\langle\alpha_s G^2\rangle$ but with an opposite sign. Given the relative smallness of the overall contribution from the gluon condensate, and the conservatively large uncertainty we have allowed in its value, the final result for m_c remains basically unchanged. This will also be true for the case of the beauty-quark mass.

3.5 Conclusion

Combining the results from both versions of the Laplace ratios, leads to the results

$$m_c(Q^2 = m_c^2) = 1.46 \pm 0.07 \text{ GeV} \tag{3.57}$$

$$m_b(Q^2 = m_b^2) = 4.70 \pm 0.07 \text{ GeV} . \tag{3.58}$$

In comparing values of m_c (or m_b) from different determinations, it is important to know which values of Λ and $\langle\alpha_s G^2\rangle$ have been used, as well as which renormalization point has been chosen, e.g. some authors determine $m_q(Q^2 = -m_q^2)$, which is related to the on-shell mass $m_q(m_q^2)$ through

$$m_q^2(m_q^2) = m_q^2(-m_q^2)(1 + \frac{4 \ln 2}{\pi}\alpha_s) . \tag{3.59}$$

After using the same values of Λ and $\langle\alpha_s G^2\rangle$ as used in [14], [16] - [21], and after converting to the on-shell mass (if necessary), we find that results from the present method are in very good agreement with those of [14] and [16], and agree within errors with [17]- [19]; the latter determinations being on the low side of our error bars. On the other hand, the technique used here gives values of m_c (or m_b) somewhat higher than those obtained in [20]- [21].

Finally, regarding the recent observation that the definition of heavy-quark pole mass in the context of the Heavy Quark Effective Theory (HQET) should contain some intrinsic ambiguity beyond perturbation theory [26], due to non-perturbative long distance effects, we notice that the hadronic system considered here is made of two heavy quarks, while HQET strictly applies to heavy-light bound states.[3] The non-relativistic ratio (3.51) is not a relation of the HQET, although it is obtained formally from the relativistic ratio (3.25) in the large quark-mass limit. The purpose of considering (3.51) together with (3.25) has been to assess the size of relativistic corrections, as well as of systematic uncertainties of QCD sum rules. The numerical results, and in particular the consistency between the relativistic and non-relativistic determinations of m_c(or m_b), indicate that these effects should be small.

Acknowledgements

I would like to thank first and foremost my supervisor, Professor C.A. Dominguez for his expert advice and endless patience in guiding me through this thesis. Thanks also goes to Joan Parsons for making the institute that much friendlier.

I would also like to thank the Foundation for Research Development for financial assistance over the past two years.

[3]An application of heavy quark symmetry to a heavy quark-antiquark system has been presented in [27].

Appendix A

Whittaker Functions

A.1 The Whittaker function

The Whittaker functions are related to the confluent hypergeometric functions

$$F(n, b, n + c, \rho) = \frac{\Gamma(n + c)}{\Gamma(n)\Gamma(c)} \int_0^1 dt\ (1 - t)^{n-1} t^{c-1} (1 - \rho + t\rho)^{-b} \tag{A.1}$$

and in the limiting case of $n \to \infty$,

$$F(n, b, n + c, \rho) = \lim_{n\to\infty} n^b G(b, c, \omega) \tag{A.2}$$

where $G(b, c, \omega)$ is the Whittaker function, and is given by.

$$G(b, c, \omega) = \frac{1}{\Gamma(c)} \int_0^1 dt\, e^{-t} t^{c-1} (\omega + t)^{-b}. \tag{A.3}$$

Furthermore, the Whittaker function (A.3) has nice derivative and asymptotic properties

$$-\frac{d}{d\omega} G(b, c, \omega) = bG(b + 1, c, \omega) \tag{A.4}$$

$$G(b, c, \omega) = \lim_{\omega\to\infty} \omega^{-b}. \tag{A.5}$$

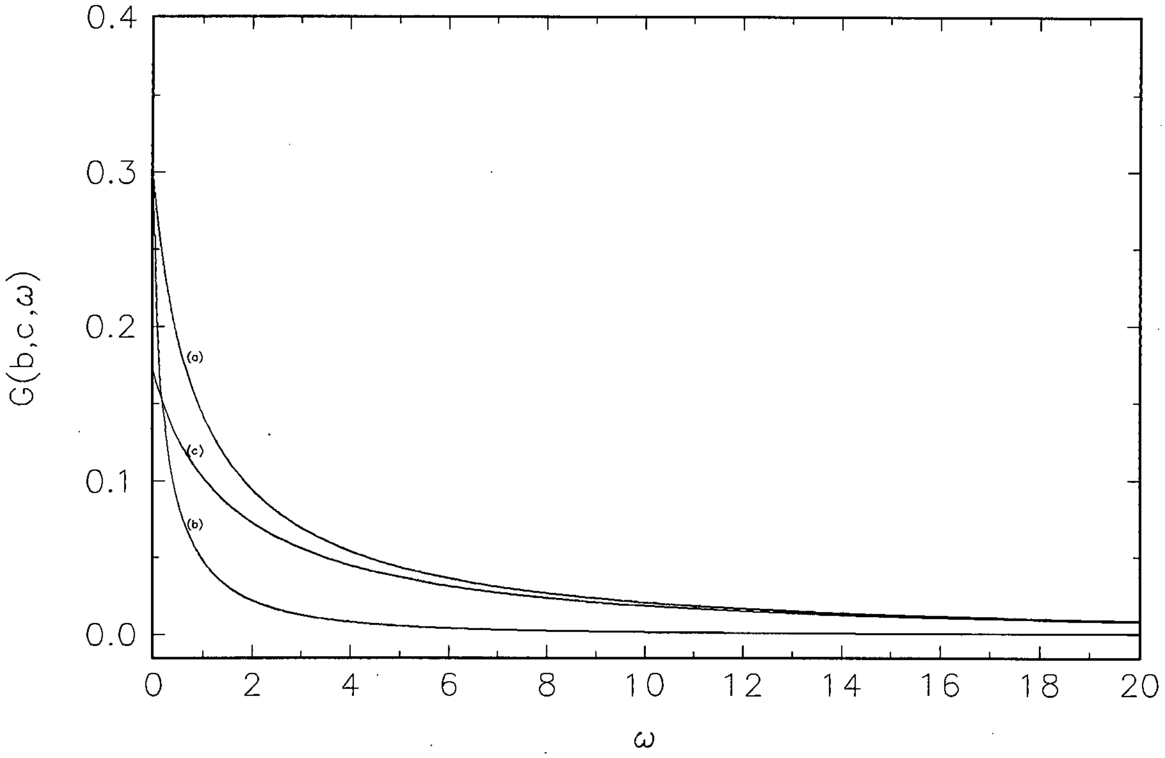

Figure A.1: The Whittaker function for parameter values: b=1.5, c=3.5 (curve(a)); b=2.5, c=3.5 (curve (b)) and b=1.5, c=4.5 (curve (c)).

A.2 Approximation for large ω

The expression (A.5) is a rather crude approximation and gives rather poor results for $\omega < 10$. [1] For this reason, a more useful expression can be derived in the following way

$$
\begin{aligned}
G(b,c,\omega) &= \frac{1}{\Gamma(c)} \int_0^\infty dt\, e^{-t} t^{c-1} (\omega + t)^{-b} \\
&= \frac{1}{\Gamma(c)} \int_0^\infty dt\, e^{-t} t^{c-1} (\omega + \omega_0 + t - \omega_0)^{-b} \\
&= \frac{1}{\Gamma(c)} (\omega + \omega_0)^{-b} \int_0^\infty dt\, e^{-t} t^{c-1} \left(1 + \frac{t-\omega_0}{\omega+\omega_0}\right)^{-b} \\
&= \frac{1}{\Gamma(c)} (\omega + \omega_0)^{-b} \int_0^\infty dt\, e^{-t} t^{c-1} \sum_{n=0}^{\infty} (-1)^n \frac{\Gamma(b+n)}{\Gamma(b)\, n!} \left(\frac{t-\omega_0}{\omega+\omega_0}\right)^n \\
&= \frac{1}{\Gamma(c)} (\omega + \omega_0)^{-b} \int_0^\infty dt\, e^{-t} t^{c-1} \left[1 - b\left(\frac{t-\omega_0}{\omega+\omega_0}\right) + \frac{b(b+1)}{2}\left(\frac{t-\omega_0}{\omega+\omega_0}\right)^2 - \ldots\right] \\
&= (\omega + \omega_0)^{-b} \left[1 - b\left(\frac{c-\omega_0}{\omega+\omega_0}\right) + \frac{b(b+1)}{2} \frac{c(c+1) - 2\omega_0 c + \omega_0^2}{(\omega+\omega_0)^2} - \ldots\right].
\end{aligned}
\tag{A.6}
$$

Now suppose we choose $\omega_0 \equiv c$, then notice that the leading correction vanishes, thus resulting in a faster convergence. Our first analytical approximation to (A.3) is

$$
G(b,c,\omega) \approx (\omega + c)^{-b} \left[1 + \frac{b(b+1)}{2} \frac{c}{(\omega+c)^2}\right]
\tag{A.7}
$$

where the analytical expressions is within 99.9% of the actual numerical value!

A.3 Recurrence relations

Besides having nice asymptotic and derivative properties, the Whittaker functions also satisfy several recurrence relations. This recurrence relations are given in [28] for the Whittaker functions

[1] In our application where the charm- and beauty-quarks masses are calculated, $\omega < 10$.

$$U(c,b,\omega) = \frac{1}{\Gamma(c)} \int_0^1 dt\, e^{-\omega t} t^{c-1} (1+t)^{b-c-1} \tag{A.8}$$

which through a simple derivation, are related to the Whittaker functions (A.3) by

$$U(c,b,\omega) = \omega^{1-b} G(-b+c+1,c,\omega) . \tag{A.9}$$

The recurrence relations for $U(c,b,\omega)$ are

$$U(c,b,\omega) = \omega^{1-b} U(1+c-b,2-b,\omega) \tag{A.10}$$

$$U(c-1,b,\omega) + (b-2c-\omega) U(c,b,\omega) + c(1+c-b) U(c+1,b,\omega) = 0 \tag{A.11}$$

$$(b-c) U(c,b,\omega) + U(c-1,b,\omega) - \omega U(c,b+1,\omega) = 0 \tag{A.12}$$

corresponding to the recurrence relations

$$G(b,c,\omega) = \omega^{c-b} G(c,b,\omega) \tag{A.13}$$

$$G(3-b,c-2,\omega) + (4-c-b-\omega) G(b-2,c-1,\omega) + (c-1)(b-2) G(b,c,\omega) = 0 \tag{A.14}$$

$$-bG(b+1,c,\omega) + G(b,c-1,\omega) - G(b,c,\omega) = 0 \tag{A.15}$$

for $G(b,c,\omega)$.

Bibliography

[1] J.D. Bjorken and S.D. Drell, Relativistic Quantum Mechanics, McGraw-Hill Book Company (1964) 1.

[2] F.J. Yndurain, Quantum Chromodynamics, Springer-Verlag (1983) 1.

[3] E. de Rafael, Lecture Notes in Physics, Vol. 118: Quantum Chromodynamics, Springer-Verlag (1980) 1.

[4] G. 't Hooft and M. Veltman, Nucl. Phys. **B 44** (1972) 189.

[5] P.H. Frampton, Gauge Field Theories, Benjamin Cummings Publishing Co. (1987) 160.

[6] C.G. Bollini and J.J. Giambiagi, Nuovo Cim. **12 B** (1972) 20.

[7] P. Pascual and R. Tarrach, QCD: Renormalization for the practitioner, Springer-Verlag (1984) 1.

[8] M.A. Shifman, A.I. Vainshtein and V.I. Zakharov, Nucl. Phys. **B 147** (1979) 385, 448.

[9] F.J. Yndurain, Phys. Lett. **63 B** (1978) 211.

[10] R. A. Bertlmann *et al.*, Z. Phys.- Particles and Fields- **C 39** (1988) 231.

[11] C.A. Dominguez and J. Solá, Z. Phys.- Particles and Fields - **C 40** (1988) 63.

[12] L.J. Reinders, H.R. Rubinstein and S. Yazaki, Nucl. Phys. **B 186** (1981) 109.

[13] J. Schwinger, Particles, sources, and fields, Vol. II (Addison-Wesley, Reading, MA, 1973).

[14] R.A. Bertlmann, Nucl. Phys. **B 204** (1982) 387.

[15] Particle Data Group, K. Hikasa *et al.*, Phys. Rev. **D 45** (1992) 1.

[16] S. Narison, Phys. Lett. **B 197** (1987) 405.

[17] J. Marrow, J. Parker and G. Shaw, Z. Phys. - Particles and Fields - **C 37** (1987) 103.

[18] J. Gasser, and H. Leutwyler, Phys. Rep. **C 87** (1982) 77.

[19] L.J. Reinders, H.R. Rubinstein and S. Yazaki, Phys. Rep. **C 127** (1985) 1.

[20] V.A. Novikov *et al.*, Phys. Rep. **41 C** (1978) 1.

[21] K.J. Miller, and M. G. Olsson, Phys. Rev. **D 25** (1982) 1247.

[22] R.A. Bertlmann, Phys. Lett. **B 116** (1982) 183.

[23] C.A Dominguez, and N. Paver, Phys. Lett. **B 293** (1992) 197.

[24] J.S. Bell and R.A. Bertlmann, Nucl. Phys. **B 177** (1981) 218.

[25] D.J. Broadhurst *et al.*, Open University Report No. OUT- 4102 - 49 (March 1994).

[26] I.I. Bigi, M.A. Shifman, N.G. Uraltsev, and A.I. Vainshtein, CERN Report No. CERN-TH.7171/94 (1994).

[27] E. Jenkins, M. Luke, A.V. Manohar and M.J. Savage, Nucl. Phys. **B 390** (1993) 463.

[28] M. Abramowitz and I. A. Stegun, Handbook of Mathematical Functions (Dover, New York, 1972).